

# Broad-band diffuse gamma ray emission of the galactic disk

F.A. Aharonian<sup>1</sup> and A.M. Atoyan<sup>2</sup>

<sup>1</sup> Max-Planck-Institut für Kernphysik, Postfach 103980, 69029 Heidelberg, Germany

<sup>2</sup> Yerevan Physics Institute, Alikhanian Br. 2, 375036 Yerevan, Armenia

Received 12 November 1999 / Accepted 31 August 2000

**Abstract.** The contributions of different radiation mechanisms to the diffuse  $\gamma$ -ray emission of the galactic disk are studied in a broad energy region from  $10^4$  to  $10^{14}$  eV. Our analysis shows that at energies between 1 and 100 MeV the radiation is dominated by the bremsstrahlung of relatively low energy, typically less than 1 GeV electrons, but with a non-negligible contribution from the inverse Compton (IC) scattering of higher energy electrons. Also, a significant fraction of the radiation observed at energies around 1 MeV could be contributed by mildly relativistic positrons annihilating “in flight” with the ambient thermal electrons. At energies from 100 MeV to 100 GeV the  $\gamma$ -ray flux is dominated by interactions of cosmic ray protons and nuclei with the ambient gas through production and subsequent decay of secondary  $\pi^0$ -mesons. The interpretation of the GeV  $\gamma$ -ray emission of the inner Galaxy as a truly diffuse radiation requires a substantially harder spectrum of relativistic protons and nuclei in the interstellar medium compared with the local cosmic ray spectrum measured directly in the solar neighborhood. In the very high energy domain,  $E_\gamma \geq 100$  GeV, the contribution of the IC component of radiation may become comparable with, or even could exceed the fluxes of  $\pi^0$ -decay component if the energy spectrum of electrons injected into the interstellar medium extends well beyond 1 TeV. Another signature of multi-TeV electrons is the synchrotron radiation which could account for a significant fraction of the diffuse hard X-ray flux of the galactic ridge. The future detailed studies of spatial and spectral characteristics of  $\gamma$ -ray emission of the galactic disk, especially at very high energies around 100 GeV by GLAST, and hopefully also at TeV energies by planned ground-based instruments should provide important insight into the understanding of the sites and mechanisms of acceleration of galactic cosmic rays and the character of their propagation in the interstellar magnetic fields.

**Key words:** radiation mechanisms: non-thermal – ISM: cosmic rays – Galaxy: general – gamma rays: theory

## 1. Introduction

Diffuse  $\gamma$ -ray emission of the galactic disk carries unique information about the fluxes and the spatial distribution of galactic

cosmic rays (CRs). Therefore it is believed that the solution of the long-standing problem of the origin of galactic CRs essentially depends on the success of observational gamma-ray astronomy. Indeed, the separation of the radiation components associated with the electronic and nucleonic components in a broad energy region from 1 MeV to 100 TeV would allow determination of the fluxes and energy spectra of CRs in different parts of the galactic disk, and thus would provide an important insight to the character of propagation of CRs in the interstellar medium (ISM). A proper understanding of the latter is a necessary condition for accurate estimates of the luminosity of the Galaxy in CRs. Our present knowledge about the propagation of CRs is based on conclusions derived from the interpretation of the mass composition and the content of the secondary anti-particles (positrons, antiprotons) of the *locally* observed CRs. Although rather effective (see e.g. Swordy 1993, Strong et al. 2000), this method requires a number of *model-dependent* assumptions. Moreover, it is not yet obvious that the locally observed CRs could be taken as undisputed representatives of the whole galactic population of relativistic particles. For example, Erlykin et al. (1998) recently argued that the fluxes of CRs could be dominated by a single or few local sources/accelerators. This statement is certainly true at least for the observed  $\geq 1$  TeV electrons which suffer severe synchrotron and IC energy losses, and thus could reach us, for any reasonable diffusion coefficient, only from the sites no farther than a few hundred parsecs (Nishimura et al. 1980, Aharonian et al. 1995).

Therefore the diffuse galactic  $\gamma$ -rays seem to be the best carriers of information about the production sites and propagation of accelerated charged particles in the galactic disk (see e.g. Ramana Murthy & Wolfendale 1993). It should be noted that the diffuse non-thermal synchrotron radiation of the ISM at radio and possibly also at X-ray wavelengths provide an additional and complementary information, but it concerns only the *electronic* component of CRs in two extreme energy bands below 1 GeV and above 100 TeV, respectively.

The extraction of the truly diffuse  $\gamma$ -ray emission, i.e. the radiation produced by CR electrons, protons and nuclei interacting with the ambient interstellar gas and photon fields, is not an easy task because of a non-negligible contamination due to weak but numerous unresolved discrete sources. Before the launch of the Compton Gamma Ray Observatory (GRO) the

Send offprint requests to: Felix.Aharonian@mpi-hd.mpg.de

information about the diffuse galactic  $\gamma$ -ray background was essentially limited to the energy region between 100 MeV and few GeV obtained by the SAS-2 (Fichtel et al. 1975) and COS B (Mayer-Hasselwander et al. 1982)  $\gamma$ -ray missions. The observations and theoretical models based on the results of these satellites were comprehensively reviewed by Bloemen (1989). In brief, these data have revealed a good correlation between the high energy  $\gamma$ -ray fluxes and the column density of the interstellar hydrogen which was a demonstration of the existence of a truly diffuse galactic gamma radiation.

The observations of the diffuse  $\gamma$ -ray background conducted in 90's by the OSSE, COMPTEL, and EGRET detectors aboard Compton GRO resulted in good quality data over five decades in energy of  $\gamma$ -rays (see Hunter et al. 1997a, and references therein). These results initiated extensive theoretical studies of different  $\gamma$ -ray production mechanisms in the ISM (e.g. Bertsch et al. 1993, Giller et al. 1995, Fathoohi et al. 1995, Gralawicz et al. 1997, Mori 1997, Porter & Protheroe 1997, Moskalenko & Strong 2000, Strong et al. 2000, Pohl & Esposito 1998).

In this paper we report the results of our study of different  $\gamma$ -ray production processes in the ISM. We discuss the fluxes of diffuse non-thermal galactic radiation of both nucleonic and electronic origin in a very broad energy region from hard X-rays to ultra-high energy  $\gamma$ -rays. Although at the first glance the problem seems to be very complicated and confused because of several competing production mechanisms, the existing data of diffuse galactic  $\gamma$ -radiation do allow rather definite conclusions concerning the relative contributions of different production processes in each specific energy band of  $\gamma$ -rays. A separate interest represents the diffuse  $\gamma$ -radiation in the very high energy (VHE) domain. In this paper we limit our study by the diffuse radiation of the *inner part* of Galaxy at  $315^\circ \leq l \leq 45^\circ$ . The inner Galaxy is not only the experimentally best studied region in diffuse  $\gamma$ -rays, but also, it presents a prime interest because of an enhanced, as currently believed, spatial concentration of CR sources in the central part of the Galaxy. We emphasize the importance of the multiwavelength approach in solution of the problem, and predict a range of  $\gamma$ -ray fluxes which could be examined by forthcoming satellite-borne and ground based  $\gamma$ -ray detectors.

## 2. The spectra of cosmic rays in the inner Galaxy

We consider a model that assumes diffusive propagation of relativistic protons/nuclei and electrons in the Galaxy. We will compare our model calculations with observations of the diffuse  $\gamma$ -radiation of the galactic disc at  $|b| \leq 5^\circ$ . Thus, although the halo of galactic CRs may extend up to heights of a few kpc (e.g. see Berezhinsky et al. 1990, Bloemen et al. 1993), we will need to know the *mean* spectrum of CRs only in a region close to the galactic plane. We approximate this region as a disk with a half-thickness  $h \simeq 1$  kpc, and a surface  $S_{\text{tot}} \approx 2S_G$ , where  $S_G = \pi R_G^2$ , and  $R_G \sim 15$  kpc is the mean radius of the Galaxy.

An important parameter for calculations of the diffuse  $\gamma$ -radiation is the mean line-of-sight depth  $l_d$  in the direction of the inner Galaxy, which basically represents the central part of

the galactic disk, with some radius  $R_d \leq R_\odot$ , where  $R_\odot \simeq 8.5$  kpc is the distance of the Sun from the center of the Galaxy. Because the densities of the gas and photon fields in the inner Galaxy are generally estimated to be significantly higher than at galactocentric distances  $R \geq R_\odot$ , the inner galactic disk should be responsible for most of the diffuse flux detected at low galactic latitudes, neglecting even the effect of a possible gradient of CR density towards the center of the Galaxy. Thus, the mean value of  $l_d$  can be reasonably estimated as  $\sim 15$  kpc.

The diffusion equation for the energy distribution  $f \equiv f(\mathbf{r}, E, t)$  of relativistic particles can be written in a general form as (Ginzburg & Syrovatskii 1964):

$$\frac{\partial f}{\partial t} = \text{div}_{\mathbf{r}}(D \text{grad}_{\mathbf{r}} f) - \text{div}_{\mathbf{r}}(\mathbf{u}f) + \frac{\partial}{\partial E}(Pf) + A[f], \quad (1)$$

where  $\mathbf{u} \equiv \mathbf{u}(\mathbf{r})$  is the fluid velocity of the gas containing relativistic particles, and  $P \equiv P(\mathbf{r}, E) = -dE/dt$  describes their total energy losses where we include also the adiabatic energy loss term  $P_{\text{adb}} = \text{div}_{\mathbf{r}} \mathbf{u}E/3$  (e.g. Owens & Jokipii 1977, Lerche & Schlickeiser 1982).  $D \equiv D(\mathbf{r}, E)$  is the spatial diffusion coefficient, and  $A[f]$  is a functional standing for various acceleration terms of relativistic particles (i.e. the sources of CRs).

The integration of Eq. (1) over the volume  $V = 2hS_G$  results in a convenient equation for the total energy distribution function of particles  $N(E, t) = \int f d^3r$  in the Galactic disk at the heights  $|z| \leq h$ . The term  $\partial f/\partial t$  leads to  $\partial N/\partial t$ . The volume integral of the two first terms in the right hand side of Eq. (1) results in:

$$\int_V [\text{div}_{\mathbf{r}}(D \text{grad}_{\mathbf{r}} f) - \text{div}_{\mathbf{r}}(\mathbf{u}f)] d^3r = \oint_{S_{\text{tot}}} D(\mathbf{e} \text{grad}_{\mathbf{r}} f) ds - \oint_{S_{\text{tot}}} (\mathbf{e} \mathbf{u}) f ds. \quad (2)$$

Here  $\mathbf{e}$  is a unit vector perpendicular to the surface element  $ds$  directed outward from the disk. These terms describe the diffusive and convective escape of particles from the disk through its surface  $S_{\text{tot}} \approx 2S_G$ .

The first surface integral in Eq. (2) can be simplified if we take into account that the CR density at heights  $z \leq h \simeq 1$  kpc, where the diffusion dominates (see below), may be significantly higher than at  $z > h$ , and approximate  $(\mathbf{e} \text{grad} f) \simeq -n(E, t)/\Delta x$ , where  $n(E, t) \equiv \bar{f}(E, t)$  is the volume averaged energy distribution function of relativistic particles, and  $\Delta x \equiv \Delta x(E)$  is the characteristic thickness of the transition layer describing the decline (i.e. the gradient) of the density of particles at energy  $E$ . Taking into account that the total energy distribution of particles  $N(E, t) = 2hS_G n(E, t)$ , one finds

$$\oint_{S_{\text{tot}}} D(\mathbf{e} \text{grad} f) = -\frac{n \bar{D} 2S_G}{\Delta x} = -\frac{N}{\tau_{\text{dif}}}, \quad (3)$$

where  $\tau_{\text{dif}}$  has a meaning of a characteristic diffusive escape time of relativistic particles from the Galactic disk:

$$\frac{1}{\tau_{\text{dif}}(E)} = \frac{\overline{D}(E)}{h\Delta x(E)}, \quad (4)$$

Here  $\overline{D}(E)$  corresponds to the mean diffusion coefficient  $D_{\text{r}}(\mathbf{r}, E)$  on the surface  $S_{\text{G}}$  of the disk.

The second surface integral in Eq. (2) can be reduced to the form  $-N(E, t)/\tau_{\text{conv}}$ , which describes a convective escape of particles from the disk through its surface due to the galactic wind driven by the pressure of CRs and of the thermal gas (e.g. Bloemen et al. 1993, Breitschwerdt et al. 1993, Zirakashvili et al. 1996):

$$\tau_{\text{conv}} \simeq ah/u. \quad (5)$$

Here  $u$  is the wind velocity on the surface of the Galactic disk which could reach  $\sim 50 \text{ km s}^{-1}$  (Zirakashvili et al. 1996) at the height  $h = 1 \text{ kpc}$ . Thus, the *mean* convective escape time of CRs from the Galactic disk can be estimated as  $\tau_{\text{conv}} \simeq 2 \times 10^7 a \text{ yr}$

The parameter  $a$  in Eq. (5) is the ratio of the mean density  $n(E)$  of particles in the disk (i.e. an average over  $-h \leq z \leq h$ ) to their density  $f(h, E)$  at the disk surface,  $z = \pm h$ . Therefore one could expect that  $a \geq 1$  and generally it may be energy-dependent as well,  $a = a(E)$ . Calculations of the spatial and energy distribution  $f(z, E)$  of the galactic CRs in the framework of the diffusion-convection model show (Lerche & Schlickeiser 1980; see also Lerche & Schlickeiser 1982, Bloemen et al. 1993) that at elevations  $z \ll z_{\text{c}}(E)$ , where  $z_{\text{c}}(E)$  is a characteristic height of the diffusion dominated region for particles with energy  $E$ , the spatial density  $f(z, E)$  is almost independent of  $z$ . Thus, at energies  $E \geq E_*$ , where  $E_*$  is found from the equation  $z_{\text{c}}(E) = h$ , the parameter  $a \sim 1$ . In the approximation  $u(z) = v_0 z$  for the galactic wind speed and  $D(E) \propto E^{\delta_1}$  with  $\delta_1 \leq 1$  for the diffusion coefficient, the height  $z_{\text{c}} = \sqrt{2D(E)/v_0(1 + \delta_1/6)}$  (see e.g. Bloemen et al. 1993). This is basically the height at which the characteristic time scale of the diffusive propagation  $\sim z^2/D$  equals the convection time scale  $v_0^{-1}$ . The energy  $E_*$  can be estimated of order of a few GeV, taking into account that at these energies  $D \sim 10^{28} \text{ cm}^2 \text{ s}^{-1}$  (e.g. Berezhinsky et al. 1990) and that  $v_0 \sim 50 \text{ km s}^{-1} \text{ kpc}$  (e.g. Zirakashvili et al. 1996), which result in  $z_{\text{c}} \simeq 1 \text{ kpc}$ .

In the convection dominated region,  $z \gg z_{\text{c}}(E)$ , the spatial density of particles starts to decline as  $f(z, E) \propto (z/z_{\text{c}})^{-\kappa}$  with  $\kappa \simeq 1.3-1.4$  (see Lerche & Schlickeiser 1992, Bloemen et al. 1993), thus  $f(h, E)/f(0, E) \propto E^{-\kappa\delta_1/2}$ . Therefore at energies  $E \ll E_*$  the parameter  $a$  should gradually increase, and in principle could be approximated as  $a(E) \propto (E/E_*)^{-\lambda}$ , with an exponent  $\lambda$  much smaller than  $\kappa\delta_1/2$  because at these energies the mean particle density  $n(E)$ , as compared with  $f(0, E)$ , should also decline. However, taking into account that  $\lambda$  is significantly less than 1, and in order to avoid an introduction of an additional model parameter, below we approximate the convective escape time as energy-independent, i.e. with  $a(E) \sim 1$  at all energies. For the CR proton component this approximation

is well justified, because for  $E_*$  of order of a few GeV the energy region  $E \ll E_*$  effectively corresponds to sub-relativistic protons which do not represent an interest for this study. Such a simplification appears reasonable also for CR electrons, because at energies  $E \ll 1 \text{ GeV}$  the spectral modifications of the electrons are defined mainly by their Coulomb energy losses which take place on time scales significantly shorter than the escape losses.

The volume integral of the third term on the right side of Eq. (1) describes the volume-averaged energy losses of the electrons with the rate  $\overline{P}(E)$ . At last, the volume integral of the 4th term in Eq. (1) describes the sources of accelerated particles  $Q(E, t)$  inside the volume  $V$ . The final equation for the overall distribution of electrons then reads:

$$\frac{\partial N}{\partial t} = \frac{\partial(\overline{P}N)}{\partial E} - \frac{N}{\tau_{\text{esc}}} + Q. \quad (6)$$

Here  $\tau_{\text{esc}}$  is the “diffusive + convective” escape time of particles:

$$\tau_{\text{esc}}(E) = \left[ \frac{1}{\tau_{\text{dif}}(E)} + \frac{1}{\tau_{\text{conv}}} \right]^{-1}. \quad (7)$$

The range of actual energy dependence of  $\tau_{\text{esc}}$  is limited at high energies because the diffusive escape time cannot be less than the light travel time  $h/c$ . This obvious requirement formally follows from the condition that the characteristic length-scale  $\Delta x(E)$  for spatial gradients in the distribution function  $f(z, E)$  cannot be less than the mean electron scattering path  $\lambda_{\text{sc}}(E)$ , otherwise the diffusion approximation implied in Eq. (1) fails. Taking into account that for relativistic particles  $D \sim \lambda_{\text{sc}}c/3$ , from Eq. (4) we find that indeed  $\tau_{\text{dif}}(E) \geq \tau_{\text{min}} \simeq 3h/c$ . The diffusive escape time can be then presented in the form

$$\tau_{\text{dif}}(E) = \tau_{10} (E/E_{10})^{-\delta} + \tau_{\text{min}}, \quad (8)$$

where  $E_{10} \equiv 10 \text{ GeV}$ . Since  $\tau_{\text{dif}}$  increases for decreasing  $E$ ,  $\tau_{\text{esc}}$  given by Eq. (7) becomes energy *independent* below some  $E_*$  when  $\tau_{\text{dif}}(E_*) = \tau_{\text{conv}}$ . Neglecting at these energies  $\tau_{\text{min}}$  in Eq. (8), from Eq. (7) then follows that in the case of a power-law approximation for  $\tau_{\text{dif}}(E)$  as in Eq. (8) the overall escape time can be presented in the form  $\tau_{\text{esc}} \approx \tau_{\text{conv}}/[1 + (E/E_*)^{\delta}]$ .

Note that generally the power-law index  $\delta$  in Eq. (8) for the diffusive escape time in the Leaky-box type Eq. (6) should be smaller than the index  $\delta_1$  of the diffusion coefficient  $D(E) \propto E^{\delta_1}$ . Since a faster diffusion of more energetic particles tends to smooth out the gradients of the distribution function  $f(z, E)$  more effectively, the characteristic length-scale  $\Delta x(E)$  would increase with energy. For a power-law approximation  $\Delta x(E) \propto E^{\delta_2}$  the index  $\delta_2 > 0$ , therefore from Eq. (4) follows that  $\delta = \delta_1 - \delta_2 < \delta_1$ . This consideration may help to qualitatively understand a formal discrepancy between CR spectral modifications due to particle propagation effects predicted in the framework of simplified Leaky-box models and more accurate diffusion-convection propagation models. Calculations for the latter models show (e.g. Lerche & Schlickeiser 1980, Bloemen et al. 1993) that at elevations  $z \ll z_{\text{c}}(E)$ , where the diffusive propagation dominates over convection, the initial power-law

spectrum of injected particles,  $Q(E) \propto E^{-\Gamma_0}$ , steepens by a factor  $\propto E^{-\delta_1}$ , whereas at  $z \gg z_c$  the increase of the effectiveness of the convective propagation results (in the case of negligible energy losses) in a steepening to only a half of the power-law exponent of the diffusion coefficient,  $f(z, E) \propto E^{-\Gamma_0 - \delta_1/2}$ . Meanwhile, the (diffusive) escape losses in the Leaky-box models result in a single power-law spectrum  $n(E) \propto E^{-\Gamma_0 - \delta}$ . Such a difference between the predictions of the CR spectra in the framework of diffusion-convection models and Leaky-box type models could be qualitatively explained, if we take into account that  $n(E)$  represents the mean particle spectrum integrated over  $z \leq h$ , which is therefore contributed (in fractions varying with  $E$ ) by both ‘diffusion’ and ‘convection’ dominated regions. Thus, the power-law index  $\delta$  for the escape time should be effectively in the region  $\delta_1/2 < \delta < \delta_1$ .

Assuming a time-dependent injection function  $Q(E, t)$ , Eq. (6) can be used for determination of the overall energy distribution of relativistic particles in a general case of a non-stationary source. If the energy losses are independent of time, the solution to this equation, in terms of spatial density functions  $n = N/V$  and  $q = Q/V$ , reads:

$$n(E, t) = \frac{1}{P(E)} \int_0^t P(\zeta_t) q(\zeta_t, t_1) \times \exp\left(-\int_{t_1}^t \frac{dx}{\tau_{\text{esc}}(\zeta_x)}\right) dt_1. \quad (9)$$

Here the variable  $\zeta_t$  corresponds to the energy of a particle at an instant  $t_1 \leq t$  which has the energy  $E$  at the instant  $t$ , and is determined from the equation

$$t - t_1 = \int_{E_e}^{\zeta_t} \frac{dE_1}{P(E_1)}. \quad (10)$$

For a quasi-stationary injection of electrons into the ISM on time-scales exceeding the escape time  $\tau_{\text{esc}}(E)$  the energy distribution of particles becomes time-independent.

For calculations of the energy distribution of CR protons in the Galaxy we take into account the energy losses connected with their inelastic interactions with the ISM gas, and the adiabatic losses of particles in a gradually accelerating wind. In a simple approximation  $u(z) \propto z$ , used e.g. by Lerche & Schlickeiser (1982) and Bloemen et al. (1993), the mean adiabatic energy loss term  $\bar{P}_{\text{adb}}(E)$  is found after a simple integration

$$2S_G \int_0^h \frac{1}{3} \frac{\partial u}{\partial z} f(z, E) dz \simeq N(E) E \frac{u(h)}{3h}$$

in the volume of the disk with  $|z| \leq h$ . This expression corresponds to  $\bar{P}_{\text{adb}} = E/\tau_{\text{adb}}$  with  $\tau_{\text{adb}} = 3h/u(h) \simeq 6 \times 10^7$  yr for  $u(h = 1 \text{ kpc}) \simeq 50 \text{ km s}^{-1}$ .

For the energy losses of particles due to their interactions with the gas, which contribute to the overall energy loss term in Eq. (6), we should use the volume-averaged gas density  $\bar{n}_H = \int_0^h n_H(z) dz/h$ , where  $n_H = n_{\text{HI}} + 2 \times n_{\text{H}_2}$  is the gas density in terms of ‘H-atoms’. In order to estimate  $\bar{n}_H$ , the HI density distribution by Dickey & Lockman (1990) can be taken: a sum of two Gaussians with central densities  $\simeq 0.4$

and  $\simeq 0.11 \text{ cm}^{-3}$  and FWHMs of 210 pc and 530 pc, respectively, and an exponential with the central density  $0.064 \text{ cm}^{-3}$  and a scale height  $\simeq 400$  pc. The molecular gas layer can be approximated by a further Gaussian with the mid-plane density  $0.3 \text{ H}_2/\text{cm}^3$  and dispersion 70 pc (Bloemen 1987). Such a gas density profile results in the mean hydrogen density  $\bar{n}_H \simeq 0.15 \text{ cm}^{-3}$  in the region  $z \leq 1 \text{ kpc}$ .

An essential process which defines the spectra of both CR protons and electrons in the Galaxy is their energy dependent escape. Beside this, for calculations of the energy distribution of the electron component of CRs we take into account the ionization (Coulomb) losses which dominate the overall energy losses of CR electrons in the ISM at energies below a few 100 MeV, the adiabatic losses, the radiative (synchrotron and inverse Compton) losses, and the bremsstrahlung losses. Note that the bremsstrahlung loss term has practically the same energy dependence as the adiabatic loss term,  $\bar{P}_{\text{brem}} \simeq E\tau_{\text{brem}}^{-1}$  (neglecting a weak logarithmic increase with energy, e.g. see Ginzburg 1979), but for  $\bar{n}_H \simeq 0.15 \text{ cm}^{-3}$  the cooling time  $\tau_{\text{brem}} \sim 3 \times 10^7/\bar{n}_H$  yr exceeds the adiabatic cooling time by a factor  $\sim 3$ . Therefore for the formation of the energy spectra of CR electrons (but *not* for the radiation flux!) the bremsstrahlung losses are by a factor of 3 less effective than the adiabatic losses. At energies above several GeV the total energy losses of the electrons are dominated by the radiative energy losses due to synchrotron emission in the ISM magnetic field of order of several  $\mu\text{G}$ , and due to the IC scattering of the electrons on different diffuse target photon fields.

Besides these processes, which should be taken into account for calculations of energy distribution of CR electrons in the disk, in this paper we discuss also a possible contribution to the fluxes of diffuse galactic radiation caused by annihilation of relativistic positrons in ‘flight’ with the ambient thermal electrons. In principle, it is possible to include also this process into calculations of  $n(E)$ , considering the energy distributions for  $e^+$  and  $e^-$  separately, and introducing in the equation for  $n_+(E)$  an additional term which describes the disappearance of the positrons due to annihilation on a timescale  $\tau_{\text{ann}}(E)$ . However, this term does not have a significant impact on the formation of the spectrum  $n_+(E)$ , because at any energy the annihilation time  $\tau_{\text{ann}}(E) = (\sigma_{\text{ann}}(E)v\bar{n}_H)^{-1} \geq (\pi r_0^2 c \bar{n}_H)^{-1} \simeq 3 \times 10^7$  yr, for the mean density  $\bar{n}_H \simeq 0.15 \text{ cm}^{-3}$ , is significantly larger than both the Coulomb loss time and the escape times involved.

For both CR protons and electrons injected into interstellar medium we assume a stationary source function (per unit volume) in a ‘standard’ power-law form with an exponential cutoff at some energy  $E_0$ :

$$q(E) \propto E^{-\Gamma_0} \exp(-E/E_0). \quad (11)$$

The flux of diffuse radiation with energy  $E_\gamma$  in a given direction is defined by the unit volume emissivity  $q_\gamma(\mathbf{r}, E_\gamma)$  integrated along the line of sight:

$$J(E_\gamma) = \int \frac{q_\gamma(\mathbf{r}, E_\gamma)}{4\pi} dl = \frac{\bar{q}_\gamma(E_\gamma) l_d}{4\pi}, \quad (12)$$

where  $\bar{q}_\gamma(E_\gamma)$  is the mean emissivity, and  $l_d$  is the characteristic line-of-sight depth of the emission region.

It is convenient to describe the flux of  $\gamma$ -rays produced at interactions of CRs with the ISM gas by the emissivity per 1 H-atom (see e.g. Bloemen 1989). Then the observed intensity of  $\gamma$ -rays linearly depends on the column density  $N_H$  along the line of sight. It is worth notice that the estimate of the mean hydrogen density  $n'_H = N_H/l_d$ , which defines the mean *emissivity* along the line of sight in direction close to the galactic plane, may be somewhat higher (by a factor about 2) than the mean gas density  $\bar{n}_H$  which should be used for the calculation of the mean (at  $z \leq 1$  kpc) energy distribution of particles in Eq. (9). Such an ‘enhancement’ of  $\bar{n}'_H$  should be allowed, and could be understood if one takes into account that at low galactic latitudes the radiation fluxes due to CR interactions with the gas are not equally contributed by the entire  $z \leq 1$  kpc region, but effectively only by a fraction of this region close to the galactic plane, with a thickness of a few 100 pc, where the spatial concentrations of *both* the relativistic particles and (especially) of the ISM gas are higher than their respective mean values averaged over  $z \leq 1$  kpc. For calculations of the IC  $\gamma$ -ray fluxes the same characteristic energy densities of the diffuse galactic photon fields as for the Eq. (9) should be used, because at elevations  $z \sim 1$  kpc these densities are still approximately the same as in the Galactic plane (e.g. see Chi & Wolfendale 1991).

### 3. Diffuse gamma radiation connected with the electronic component of CRs

There are four principal processes of production of non-thermal hard X-rays and  $\gamma$ -rays in the ISM by CR electrons: inverse Compton (IC) scattering, bremsstrahlung, annihilation of positrons, as well as synchrotron radiation provided that the electrons are accelerated beyond 100 TeV. In this section we discuss the first three mechanisms; the synchrotron radiation of hard X-rays will be discussed in Sect. 5 in the context of the IC radiation of highest energy electrons.

#### 3.1. IC gamma rays

The calculations of the diffuse IC  $\gamma$ -rays require knowledge of the low-frequency target photon fields and of the flux of electrons in ISM.

The photon fields which are important for production of IC  $\gamma$ -rays in the ISM are 2.7 K cosmic microwave background radiation (MBR), and the diffuse galactic radiation contributed by the starlight and dust photons with peak intensities around  $1 \mu\text{m}$  and  $100 \mu\text{m}$ , respectively. While the density of 2.7 K MBR is universal, with  $w_{\text{MBR}} \approx 0.25 \text{ eV}/\text{cm}^3$ , the densities of diffuse galactic radiation fields vary from site to site, and actually are model dependent. Detailed calculations of Chi & Wolfendale (1991) show that the starlight energy density increases from the local value  $w_{\text{NIR}} \approx 0.5 \text{ eV}/\text{cm}^3$  (Mathis et al. 1983) up to  $\approx 2.5 \text{ eV}/\text{cm}^3$  in the central 1 kpc region of the inner Galaxy. For calculations below we use the mean value  $w_{\text{NIR}} \approx 1.5 \text{ eV}/\text{cm}^3$ . The energy density of the FIR produced

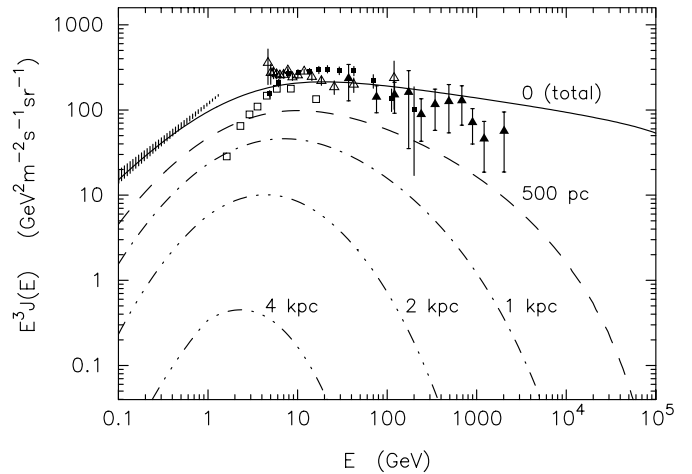


**Fig. 1.** The fluxes of CR electrons near the Sun from sources continuously and uniformly distributed in the galactic disk calculated in the framework of the diffusive propagation model for a diffusion coefficient with  $D(10 \text{ GeV}) = 10^{28} \text{ cm}^2 \text{ s}^{-1}$  and a power law index  $\delta_1 = 0.6$ , and a power-law injection spectrum of the electrons with  $\Gamma_{e,0} = 2.4$ . The total flux (solid curve,  $r_0 = 0$  pc) is decomposed in order to show the contributions from the sources located at distances  $r \geq r_0$  for different  $r_0$  indicated near the curves. The hatched region corresponds to the estimate of the mean flux of low energy electrons derived from radio data in the direction of galactic poles by Webber et al. (1980). The data points shown correspond to the local fluxes of CR electrons measured by different groups (for details see Atoyan et al. 1995)

by dust in the galactic plane is more uncertain, and is typically estimated from  $w_{\text{FIR}} \approx 0.05\text{--}0.1 \text{ eV}/\text{cm}^3$  (e.g. Mathis et al. 1983) to  $w_{\text{FIR}} \approx 0.2\text{--}0.3 \text{ eV}/\text{cm}^3$  (Chi & Wolfendale 1991). For calculations of the IC  $\gamma$ -ray fluxes below we adopt  $w_{\text{FIR}} \approx 0.2 \text{ eV}/\text{cm}^3$ . Fortunately, large uncertainties in  $w_{\text{FIR}}$  appear not crucial because at all  $\gamma$ -ray energies the contribution from IC upscattering of 2.7 K target photons significantly exceeds the IC fluxes produced on FIR (see below).

Another source of uncertainties in calculations of the fluxes of diffuse  $\gamma$ -rays is the lack of independent information about the flux and the spectrum of galactic electrons above several GeV. While radio measurements allow definite conclusions about the average electron flux below a few GeV, at higher energies the electron fluxes in the Galaxy are in principle model dependent. The standard interpretation of the energy spectrum of CRs usually assumes a uniform and continuous distribution of sources in the Galaxy both in space and time. Whereas for the nucleonic component of CRs this approximation can be considered as a reasonable working hypothesis, the validity of this assumption for the electrons is questionable at least for the high energy part of the measured spectrum which extends up to 2 TeV (Taira et al. 1993). Because of severe radiative losses, the sources of these electrons could not be located well beyond a few 100 pc (Nishimura et al. 1980, Aharonian et al. 1995), and therefore the measured electron spectrum might not be applicable for calculations of  $\gamma$ -radiation from the distant parts of the galactic disk.

In Fig. 1 the energy spectrum of CR electrons calculated assuming a uniform and continuous distribution of the sources in the galactic disk (solid curve) is decomposed to show the contributions from sources located at distances  $r \geq r_0$  for different  $r_0$ . It is seen that even at energies  $\sim 10$  GeV the total flux of the observed electrons is dominated by particles accelerated and injected into ISM at distances  $r \leq 1$  kpc from the Sun. At TeV energies the sources beyond 500 pc contribute only  $\sim 10\%$  of the total electron flux. Since for these relatively small spatial scales the assumption of continuous distribution (both in space and in time) of CR sources may not be well justified, the spectrum and the flux of high energy electrons at TeV and higher energies may show significant variations in different sites of the galactic disk (Atoyan et al. 1995). In particular, one could expect a significant enhancement of the electron fluxes in the central region of the Galaxy due to presumably higher concentration of cosmic ray sources there. Therefore we may allow deviations of the predicted electron distribution in the inner Galaxy from the observed fluxes, perhaps except for the region below few GeV where the radio observations, provide information about the average spectrum of galactic electrons along the line of sight (see also Porter & Protheroe 1997, Pohl & Esposito 1998, Strong et al. 2000). It should be noted, however, that because of a significant absorption of radio fluxes in the interstellar medium, a *direct* information about the spectra of CR electrons in the inner Galaxy is not actually available. The fluxes of radio electrons in the Galaxy are generally deduced using the observations from the directions of the galactic poles or the anticenter (e.g. see Webber et al. 1980) under an assumption of a homogeneous distribution of CRs in the galactic disk.

In Fig. 2 we show the average spectrum of electrons in the inner part of the Galaxy calculated in the framework of the model described in Sect. 2, assuming a power-law index for the electron injection spectrum  $\Gamma_{e,0} = 2.15$ , and normalizing the energy density  $w_e = \int E n(E) dE$  to  $0.05 \text{ eV/cm}^3$ . For the parameters used in calculations, this normalization requires an acceleration rate of electrons

$$L_e \simeq 1.6 \times 10^{37} \text{ erg/kpc}^3 \text{ s}. \quad (13)$$

This implies that for the inner part of the Galactic disk, with  $R \leq 8.5$  kpc and a half thickness 1 kpc, the overall acceleration power should be about  $7 \times 10^{39} \text{ erg s}^{-1}$ . In the energy region between 100 MeV and 1 GeV the energy losses of electrons are dominated by the adiabatic losses and the bremsstrahlung, with  $dE/dt \propto E$ , which do not change the original (acceleration) spectrum of electrons. Indeed, it is seen from Fig. 2 that in this energy region, which is responsible for synchrotron radio emission, the electron spectrum remains rather close to the injection spectrum. Therefore the spectral index of the observed synchrotron radio emission contains almost model-independent information about the injection spectrum of electrons. At energies below 100 MeV the electron spectrum suffers significant deformation (flattening) because of ionization losses, and at energies above 1 GeV the energy distribution of the electrons steepens because of a combination of escape and radiative (synchrotron and inverse Compton) losses.

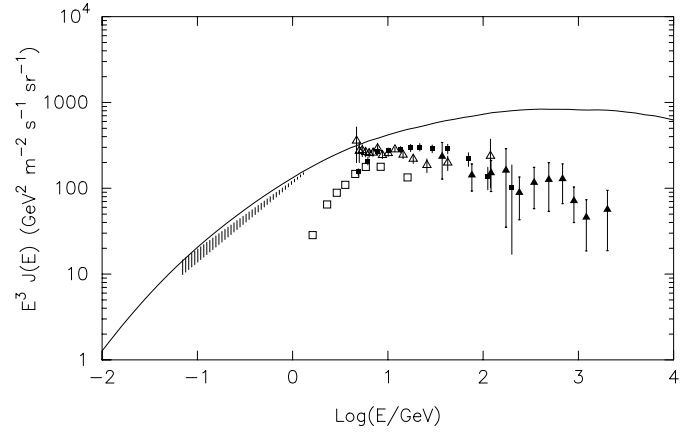


**Fig. 2.** The mean flux of electrons in the central region of the Galaxy calculated assuming a stationary injection spectrum of electrons with  $\Gamma_{e,0} = 2.15$  and  $E_0 = 100$  TeV, and the following model parameters for the escape time in Eq. (7):  $\tau_{\text{conv}} = 2 \times 10^7$  yr,  $\tau_{10} = 10^7$  yr,  $\delta = 0.6$ ,  $\tau_{\text{min}} = 3 \times 10^3$  yr. For parameters of the ISM we have assumed:  $B = 6 \mu\text{G}$ ,  $\bar{n}_{\text{H}} = 0.15 \text{ H-atom/cm}^3$  (see text), and  $w_{\text{FIR}} = 0.2 \text{ eV/cm}^3$ ,  $w_{\text{NIR}} = 1.5 \text{ eV/cm}^3$ . The injection rate of electrons is normalized so that the energy density in the resulting spectrum of CR electrons is  $w_e = 0.05 \text{ eV/cm}^3$ . The hatched region is the same as in Fig. 1

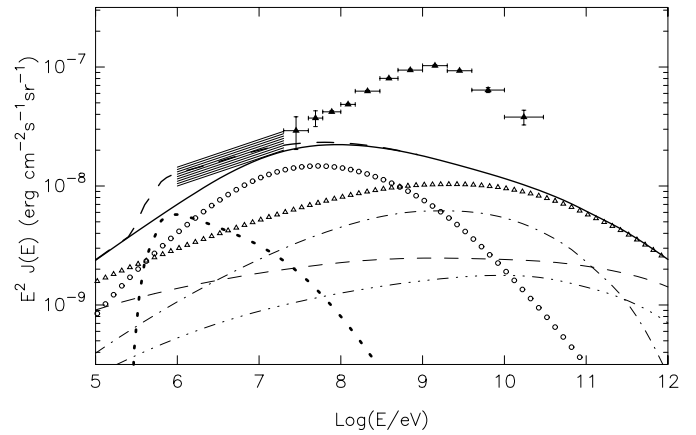


**Fig. 3.** The flux of diffuse  $\gamma$ -rays produced by the CR electrons due to different radiation processes in the inner Galaxy. For calculations we assume the characteristic line-of-sight depth of the emission region  $l_d = 15$  kpc and the gas column density  $N_{\text{H}} = 2 \times 10^{22} \text{ cm}^{-2}$ . The open dots show the bremsstrahlung flux, and the open triangles show the overall flux of the IC radiation due to different target photons: 2.7 K MBR (thin dashed line), diffuse NIR/optical radiation assuming  $w_{\text{NIR}} = 1.5 \text{ eV/cm}^3$  (dot-dashed line), diffuse FIR radiation with  $w_{\text{FIR}} = 0.2 \text{ eV/cm}^3$  (3-dot-dashed line). The heavy dotted line shows the flux of  $\gamma$ -rays due to annihilation of relativistic positrons in flight in the case of a high charge composition  $C_+ = e^+/(e^+ + e^-) = 0.5$  for electrons with energies 1–100 MeV. The sum of the bremsstrahlung and IC fluxes is shown by solid line. The heavy dashed line corresponds to the overall  $\gamma$ -ray flux including also the annihilation radiation. The data points show the mean flux of diffuse high energy  $\gamma$ -rays observed by EGRET (Hunter et al. 1997a), and the hatched region shows the range of average diffuse  $\gamma$ -ray fluxes detected by COMPTEL (Strong et al. 1997; Hunter et al. 1997b) from the direction of the inner Galaxy at low galactic latitudes.

The calculated fluxes of diffuse  $\gamma$ -rays produced by electrons are shown in Fig. 3. The spectrum of IC  $\gamma$ -rays below the highest energy observed by EGRET,  $E \leq 30$  GeV, is not very sensitive to the exact value of the cutoff energy  $E_0$  in the injection spectrum of electrons, provided that  $E_0$  exceeds 10 TeV. For the energy density of the diffuse interstellar NIR/optical radiation we have assumed  $w_{\text{NIR}} = 1.5 \text{ eV/cm}^3$ . For this value of  $w_{\text{NIR}}$  the IC radiation component produced on the galactic starlight photons (dot-dashed line) somewhat exceeds in the energy region 10 MeV - 30 GeV the IC flux produced on 2.7 K MBR (dashed line). The ‘FIR’ component of IC radiation (3-dot-dashed line) calculated for  $w_{\text{FIR}} = 0.2 \text{ eV/cm}^3$  at any  $\gamma$ -ray energy contributes less than 25% of the total IC flux.

In its turn, the overall IC  $\gamma$ -ray flux can account, for the chosen infrared photon field densities, only for  $\leq 20\%$  of the observed  $\gamma$ -ray fluxes both at MeV (“COMPTEL”) and GeV (“EGRET”) energies (see Fig. 3). For the same average electron fluxes shown in Fig. 2, the fluxes of IC radiation could be increased assuming formally a larger depth  $l_d$  of the emission region. However, the value of the mean  $l_d = 15$  kpc assumed in Fig. 3 is already large, and hardly it could be significantly increased further. Another way to increase the flux of IC  $\gamma$ -rays is possible if we assume that the energy density of the electrons in the inner Galaxy is significantly larger than  $w_e = 0.05 \text{ eV/cm}^3$ . However, for a fixed gas column density  $N_{\text{H}}$  this would automatically increase also the flux of the bremsstrahlung  $\gamma$ -rays, resulting in an overproduction of diffuse radiation in the 10–30 MeV region (see below).

The possibilities to increase the flux of IC  $\gamma$ -rays to a level significantly higher than in Fig. 3 are essentially limited also by the radio observations. The density of the Galactic electrons in the energy range 70 MeV to 1.2 GeV shown in Fig. 2 is derived by Webber et al. (1980) from radio observations at low frequencies in the galactic pole directions assuming the average magnetic field  $B \sim 6 \mu\text{G}$ . Thus, below few GeV the spectral index of electrons is well fixed,  $\Gamma_e = 2\alpha_r - 1 = 2.14 \pm 0.06$  (for the photon spectral index of the observed radio emission  $\alpha_r = 1.57 \pm 0.03$ ), but their absolute flux depends on the magnetic field.

The mean energy of the IC  $\gamma$ -rays produced by an electron with energy  $E_e$  on target photons with an energy  $\epsilon_0$  is  $E_{\text{IC}} = (4/3)(E_e/m_e c^2)^2 \epsilon_0$ . Therefore IC radiation of 1 GeV ‘radio’ electrons on the IR/optical photons with  $\epsilon_0 \sim 1\text{--}2 \text{ eV}$  corresponds to energies  $E \sim 5\text{--}10 \text{ MeV}$ . The expected energy flux,  $F(E) = E^2 J(E)$ , of these IC  $\gamma$ -rays can be estimated analytically:

$$F_{\text{IC}}^{(\text{NIR})}(E) \simeq 1.5 \times 10^{-9} \frac{w_e}{0.1 \text{ eV/cm}^3} \frac{w_{\text{NIR}}}{1 \text{ eV/cm}^3} \frac{l_d}{10 \text{ kpc}} \times \left( \frac{\epsilon_0}{1 \text{ eV}} \right)^{\frac{\Gamma_e-3}{2}} \left( \frac{E}{5 \text{ MeV}} \right)^{\frac{3-\Gamma_e}{2}} \frac{\text{erg}}{\text{cm}^2 \text{ s sr}} \quad (14)$$

for  $\Gamma_e \simeq 2.15$ . The comparison of Eq. (14) with the results of numerical calculations (the dot-dashed line in Fig. 3) shows a reasonable accuracy of this convenient analytical expression. Normalizing the flux of GeV electrons to the radio flux,  $F_\nu =$

$\nu S_\nu \simeq 10^{-10} \text{ erg/cm}^2 \text{ s ster}$  at  $\nu = 10 \text{ MHz}$ , we find a direct relation between the IC  $\gamma$ -ray fluxes produced on NIR/optical photons by GeV electrons and the *un-absorbed* radio fluxes to be expected from the inner Galaxy:

$$F_{\text{IC}}^{(\text{NIR})}(E) \simeq 2.6 \frac{w_{\text{NIR}}}{1 \text{ eV/cm}^3} \left( \frac{B}{6 \mu\text{G}} \right)^{-\frac{1+\Gamma_e}{2}} \times \left( \frac{\epsilon_0}{1 \text{ eV}} \right)^{\frac{\Gamma_e-3}{2}} \left( \frac{E}{5 \text{ MeV}} \right)^{\frac{3-\Gamma_e}{2}} F_{10 \text{ MHz}}. \quad (15)$$

For a given radio flux in the galactic plane, a decrease of the magnetic field by a factor of two would lead to an increase of the electron flux shown in Fig. 2 by a factor of  $2^{\alpha_r} \sim 3$ , and correspondingly to the increase of the IC  $\gamma$ -ray fluxes by the same factor.

Unfortunately, at low frequencies the absorption of radio fluxes from the inner Galaxy at low galactic latitudes is very significant, so the diffuse radio flux  $F_{10 \text{ MHz}}$  is uncertain. Eq. (15) predicts that this analytical estimate of the IC flux (for  $E \leq 10 \text{ MeV}$ ) would be in agreement with the results of numerical calculations shown by the dot-dashed line in Fig. 3 for the un-absorbed radio flux from the inner Galaxy  $F_{10 \text{ MHz}} \sim 4 \times 10^{-10} \text{ erg/cm}^2 \text{ s ster}$ , i.e. by a factor 5 larger than the Galactic radio flux observed in the polar directions,  $\approx 8 \times 10^{-11} \text{ erg/cm}^2 \text{ s ster}$  (Webber et al. 1980). This implies a size of the halo of the Galactic CRs extending up to heights  $\sim 3 \text{ kpc}$  (to be compared with  $l_d \sim 15 \text{ kpc}$  used in Fig. 3), which is in agreement with the relevant theoretical predictions in the framework of the diffusion models (e.g. Bloemen et al. 1993).

Fig. 3 and Eq. (14) show that any attempt to explain the observed  $\gamma$ -ray fluxes at  $E \sim 1\text{--}10 \text{ MeV}$ ,  $F_{\text{obs}} \geq 10^{-8} \text{ erg cm}^{-2} \text{ s}^{-1} \text{ sr}^{-1}$  by IC radiation either would require an energy density of the NIR/optical radiation at a level of  $\geq 5 \text{ eV/cm}^3$ , which is much larger than it is generally accepted for the density of starlight photons in the ISM, or would require a very high flux of the radio electrons in the inner Galaxy. The latter assumption would imply, however, very high radio fluxes, exceeding by more than one order of magnitude the flux detected from the direction of the Galactic poles, unless we assume a (unrealistically) low magnetic field,  $B \sim 1 \mu\text{G}$  or so, in the Galactic plane. Moreover, independently of the strength of the interstellar magnetic field, such an assumption of high flux of  $E \leq 1 \text{ GeV}$  electrons leads to a simultaneous increase and overproduction of the bremsstrahlung flux as well, which would then exceed the  $\gamma$ -ray flux observed between 1 and 100 MeV.

### 3.2. Electron bremsstrahlung

Since the bremsstrahlung  $\gamma$ -rays below 1 GeV are produced by the same electrons which are responsible also for the galactic synchrotron radio emission, the differential flux  $J(E)$  of this radiation in the region from 30 MeV to  $\sim 1 \text{ GeV}$  should have a characteristic power-law slope with an index coinciding with the spectral index of the radio electrons  $\Gamma_e \simeq 2.1\text{--}2.2$ . The results of numerical calculations are shown in Fig. 3 by open

dots. For a power-law spectrum of electrons the energy flux of bremsstrahlung  $\gamma$ -rays can be calculated analytically:

$$F_{\text{brem}}(E) \simeq 1.3 \times 10^{-8} \frac{w_e}{0.1 \text{ eV/cm}^3} \frac{N_{\text{H}}}{10^{22} \text{ cm}^{-2}} \times \left( \frac{E}{100 \text{ MeV}} \right)^{2-\Gamma_e} \frac{\text{erg}}{\text{cm}^2 \text{ s sr}}, \quad (16)$$

In calculations we have assumed a standard composition of the interstellar gas ( $\simeq 90\%$  of the molecular and atomic hydrogen, and  $\simeq 10\%$  of helium).

It is worthwhile to compare the bremsstrahlung flux in the energy region  $E \sim 30$  MeV with the ‘NIR’ component of IC flux in the region  $E \sim 10$  MeV since both components are due to the radiation of the same radio electrons, (although contributed by two different, low-energy and high-energy, parts of the power-law distribution of radio electrons, respectively). Assuming for the mean photon energy of NIR  $\epsilon_0 \simeq 1$  eV, and  $\Gamma_e = 2.15$  for the radio electrons, from Eqs. (14) and (16) we find:

$$\frac{F_{\text{brem}}(30 \text{ MeV})}{F_{\text{IC}}^{(\text{NIR})}(10 \text{ MeV})} \simeq 7.6 \frac{N_{\text{H}}}{10^{22} \text{ cm}^{-2}} \left( \frac{l_{\text{d}}}{10 \text{ kpc}} \right)^{-1} \times \left( \frac{w_{\text{NIR}}}{1 \text{ eV/cm}^3} \right)^{-1}. \quad (17)$$

Comparison of Eq. (15) with the results of numerical calculations in Fig. 3 shows a good accuracy of this analytical estimate.

In the region  $E \leq 30$  MeV the bremsstrahlung flux is due to electrons with  $E_e < 70$  MeV (i.e. outside the domain of radio emitting electrons) where ionization losses result in a significant flattening of the electron spectra  $n(E_e)$ . This results in a drop of  $F_{\text{brem}}$  at 10 MeV by a factor of 1.5 compared with  $F_{\text{brem}}(30 \text{ MeV})$ . For  $w_{\text{NIR}} = 1.5 \text{ eV/cm}^3$  assumed in Fig. 3 the overall IC flux at 10 MeV is comparably contributed by both NIR and MBR target photons. In the case of a higher density of the diffuse NIR field in the inner Galaxy the overall IC radiation at those  $\gamma$ -ray energies will be dominated by the IC upscattering of the starlight photons. Taking all these effects into account, one can conclude from Eq. (17) that at energies  $E \sim 10$  MeV the bremsstrahlung should dominate the overall diffuse emission observed in the direction of the Galactic plane, unless one assumes a very high energy density of NIR,  $w_{\text{NIR}} \geq 5 \text{ eV/cm}^3$  as adopted by Strong et al. (2000).

Independently of the density of the NIR in the inner Galaxy, a conclusion that the contribution of the bremsstrahlung to the overall flux of the galactic diffuse  $\gamma$ -ray background is large, can be derived from the comparison of the fluxes produced by the same  $70 \text{ MeV} \leq E_e \leq 1 \text{ GeV}$  electrons in the radio and  $\gamma$ -ray regions. At the photon energy 30 MeV this results in

$$F_{\text{brem}}(30 \text{ MeV}) \simeq 28 \frac{N_{\text{H}}}{10^{22} \text{ cm}^{-2}} \left( \frac{l_{\text{d}}}{10 \text{ kpc}} \right)^{-1} \times \left( \frac{B}{6 \mu\text{G}} \right)^{-1.57} F_{10 \text{ MHz}}, \quad (18)$$

where  $F_{10 \text{ MHz}}$  is an un-absorbed flux produced in the galactic plane. Since the latter cannot be less (and, presumably, is even several times higher) than the flux  $10^{-10} \text{ erg cm}^{-2} \text{ s}^{-1} \text{ sr}^{-1}$  detected from the direction of the Galactic poles (Webber et al. 1980), the contribution of the bremsstrahlung to the overall diffuse flux of  $E \sim 10$  MeV  $\gamma$ -rays should be significant, unless one would assume either a very high magnetic field ( $B \gg 10 \mu\text{G}$ ) or a very low gas column density ( $N_{\text{H}} \ll 10^{22} \text{ cm}^{-2}$ ) in the direction of the inner Galaxy.

### 3.3. Annihilation of CR positrons in flight

Since a significant fraction of the CR electron component could be in the form of positrons, a non-negligible contribution to the diffuse  $\gamma$ -radiation below 10 MeV could be due to annihilation of mildly relativistic positrons (Aharonian & Atoyan 1981a, Aharonian et al. 1983). The differential spectrum of the  $\gamma$ -rays produced at the annihilation of a fast positron with a Lorentz-factor  $\gamma_+ = E_+/m_e c^2$  on the ambient electrons with density  $n_e$  is described by a simple analytical expression (Aharonian & Atoyan 1981b)

$$q_{\text{ann}}(\epsilon) = \frac{\pi r_e^2 c n_e}{\gamma_+ p_+} \left[ \left( \frac{\epsilon}{\gamma_+ + 1 - \epsilon} + \frac{\gamma_+ + 1 - \epsilon}{\epsilon} \right) + 2 \left( \frac{1}{\epsilon} + \frac{1}{\gamma_+ + 1 - \epsilon} \right) - \left( \frac{1}{\epsilon} + \frac{1}{\gamma_+ + 1 - \epsilon} \right)^2 \right] \quad (19)$$

where  $p_+ = \sqrt{\gamma_+^2 - 1}$  is the dimensionless momentum of the annihilating positron<sup>1</sup>, and the photon energy  $\epsilon = E/m_e c^2$  varies in the limits

$$\gamma_+ + 1 - p_+ \leq 2\epsilon \leq \gamma_+ + 1 + p_+. \quad (20)$$

For the power-law spectrum of the positrons  $N_+ \propto \gamma_+^{-\Gamma_e}$ , the spectrum of annihilation radiation at high energies  $E \gg m_e c^2$  has a power-law form

$$J_{\text{ann}}(E) \propto E^{-(\Gamma_e+1)} [\ln(2E/m_e c^2) - 1]. \quad (21)$$

Thus, the spectrum of annihilation radiation is steeper than the spectrum of electrons, in contrast to the spectrum of bremsstrahlung radiation which in the high energy limit repeats the spectrum of parent electrons. At lower energies the spectrum has a more complicated form with a maximum around 1 MeV. The ratio of the fluxes  $J_{\text{ann}}/J_{\text{brem}}$  does not depend on the ambient gas density, and for a given ratio  $C_+ = e^+/(e^+ - e^-)$  depends only on the spectrum of electrons, being higher for steep electron spectra.

The flux of annihilation radiation calculated for the spectrum of electrons shown in Fig. 2, and assuming 50% content of positrons, is presented in Fig. 3. It is seen that under such an assumption the contribution of the annihilation radiation at 1 MeV exceeds the fluxes produced by all other radiation processes, including the bremsstrahlung. Therefore we conclude that depending on the (unknown) content of low-energy ( $\leq 100$  MeV)

<sup>1</sup> Note that in Aharonian & Atoyan (1981b) there is a misprint in Eq. (5), namely the momentum  $p_+$  in the denominator is missing.

positrons in CRs, this process may result in a significant enhancement of the diffuse radiation at MeV energies. Note that at energies  $E_e < 1$  GeV the fraction of positrons in the local (directly measured) component of CR electrons gradually increases, reaching  $C_+ \geq 0.3$  (although with large uncertainties) at  $E_e \sim 100$  MeV (Fanslow et al. 1969). A detailed discussion of different possibilities which may provide enhanced positron flux at low energies is out of the scope of this paper. We note only that pulsars could be potential suppliers of low-energy ( $e^+$ ,  $e^-$ ) pairs into the electronic component of CRs (see e.g. Harding & Ramaty 1987). Also, we may speculate that a moderate acceleration of beta-decay positrons produced at early stages in SNRs would result in such an enhancement. Obviously these possibilities require thorough examination, therefore the adopted in this paper large content of positrons at low energies should be considered as a *working hypothesis* which helps to explain the MeV excess in the galactic diffuse background radiation.

The assumption that the process of annihilation of suprathermal positrons in flight might significantly contribute to the diffuse low-energy  $\gamma$ -radiation of the inner Galaxy in principle would imply also a high flux of 0.511 MeV annihilation line radiation, and a rather broad continuum emission at  $E \leq 0.511$  MeV due to annihilation of the thermalized positrons through the positronium channel (Leventhal 1973). OSSE measurements (Purcell et al. 1993) have shown that the flux of the diffuse annihilation radiation detected from the inner Galaxy is dominated ( $\simeq 97\%$ , Kinzer et al. 1996) by the positronium annihilation, which consists of two components - a narrow 0.511 MeV annihilation line and the  $\gamma$ -ray continuum below 0.5 MeV. At energies  $E \sim (0.2-0.5)$  MeV the diffuse  $\gamma$ -ray emission of the inner Galaxy is contributed mainly by the fluxes of these two components of the annihilation radiation (not shown in Fig. 3; but see e.g. Hunter et al. 1997b). The total flux of these photons is at the level  $\simeq 10^{-3} \text{ cm}^{-2} \text{ s}^{-1}$  (see Kinzer et al. 1996), which is equivalent to  $\simeq 2.4 \times 10^{-2} \text{ cm}^{-2} \text{ s}^{-1} \text{ ster}^{-1}$  for the field of view  $3.8^\circ \times 11.4^\circ$  of the OSSE instrument.

Our earlier calculations (Aharonian & Atoyan 1981a) show that in the approximation of an infinite interstellar medium, about 20% of relativistic positrons would annihilate in flight on the thermal electrons of the same gas medium where they cool due to (predominantly) Coulomb and bremsstrahlung energy losses. Thus, in this case the total photon flux from the annihilation of the positrons after their thermalization in the ambient ISM would be by a factor of 4 larger than the total photon flux due the annihilation of relativistic positrons. The integrated flux of the annihilation radiation by relativistic electrons shown in Fig. 3 (dotted curve), is  $\simeq 6.7 \times 10^{-3} \text{ cm}^{-2} \text{ s}^{-1} \text{ ster}^{-1}$ . Therefore one could expect that the photon flux associated with the thermalized component of CR positrons would be as high as  $J_{0.511} \simeq 2.7 \times 10^{-2} \text{ cm}^{-2} \text{ s}^{-1} \text{ ster}^{-1}$ , provided that the positron content in the total flux of CR electrons is as high as  $C_+ = 0.5$ , as assumed in Fig. 3. This flux is quite comparable with the annihilation radiation flux observed.

We should note, however, that the ratio of CR positrons that annihilate after their thermalization to the positrons annihilating while remaining still relativistic may be in fact significantly (by

a factor of few) lower because this estimate does not take into account the escape losses of particles from the thin gaseous disk of the Galaxy. Meanwhile, the positrons, both relativistic and thermalized, escape (in particular, by convection) from the disk on timescales comparable with, and even shorter than their cooling and annihilation times, which may therefore significantly reduce (for the same high  $C_+$ ) the flux of the annihilation radiation associated with the thermalized CR positrons. This problem needs, however, a separate study which is out of the scope of the present paper.

A possible source of relativistic positrons in the energy region below 100 MeV, which presents a prime interest from the point of view of production of the continuum annihilation radiation (by relativistic positrons) and the subsequent production of the 0.511 MeV line and three-photon positronium continuum (by thermalized positrons), are interactions of CR protons and nuclei with the ambient gas via production and decay of secondary  $\pi^+$ -mesons. The total  $\gamma$ -ray flux above 100 MeV from the inner Galaxy, associated with the  $\pi^0$ -decay component of diffuse radiation, cannot significantly exceed  $\sim 10^{-4} \text{ ph/cm}^2 \text{ s sr}$  (see below), therefore it strongly limits the contribution of these positrons to the observed flux of 0.511 MeV line, and consequently also to the  $\gamma$ -ray continuum at  $E \leq 10$  MeV. Obviously a more copious mechanism for production of positrons in the Galaxy with energy  $\leq 100$  MeV is needed in order to interpret the ‘‘MeV’’ excess of the diffuse  $\gamma$ -radiation of the inner Galaxy. Ejection of relativistic electron-positron pairs from the pulsar magnetospheres seems an interesting possibility. Apparently, this question also needs a separate detailed study, which cannot be done in this paper.

The overall flux of bremsstrahlung and IC diffuse  $\gamma$ -rays is shown in Fig. 3 by solid line. It is seen that the  $\gamma$ -radiation of the CR electrons is significantly below the measured spectrum in the entire energy range from 100 MeV to 30 GeV. Due to the lack of independent information on the spectrum of high energy electrons with  $E_e \gg 1$  GeV in the inner Galaxy, the predictions of diffuse  $\gamma$ -radiation above several 100 MeV could contain significant uncertainties. Although both at 100 MeV and 30 GeV energies the deviation of the calculated fluxes from the measurements (by a factor of  $\approx 2$ ) should not be overemphasized, the gap by a factor of 5 to 7 around 1 GeV is not easy to explain by a reasonable set of model parameters. Moreover, the flat shape of the overall flux produced by CR electrons cannot explain the GeV bump without violation of the fluxes observed at lower energies. Below we study the possibility of explanation of this bump by the nucleonic component of diffuse radiation connected with interactions of CR protons and nuclei with the interstellar gas.

## 4. Gamma rays of nucleonic origin

### 4.1. Emissivity of $\pi^0$ -decay $\gamma$ -rays

Relativistic protons and nuclei produce  $\gamma$ -rays in the inelastic collisions with ambient nucleons due to production and decay of  $\pi^0$ -mesons,  $pp \rightarrow \pi^0 \rightarrow 2\gamma$ . This mechanism has been ex-

tensively studied by many authors (e.g. Stecker 1979, Dermer 1986, Berezhinsky et al. 1993, Mori 1997). Here we present a simple formalism which allows us to calculate with high accuracy the emissivity of  $\gamma$ -rays in the case of any broad energy distribution of CRs.

The emissivity  $q_\gamma(E_\gamma)$  of  $\gamma$ -rays due to decay of  $\pi^0$ -mesons is directly defined by their emissivity  $q_\pi(E_\pi)$  as

$$q_\gamma(E_\gamma) = 2 \int_{E_{\min}}^{\infty} \frac{q_\pi(E_\pi)}{\sqrt{E_\pi^2 - m_\pi^2 c^4}} dE_\pi, \quad (22)$$

where  $E_{\min} = E_\gamma + m_\pi^2 c^4 / 4E_\gamma$ , and  $m_\pi$  is the  $\pi^0$ -meson rest mass.

The emissivity of secondary particles from inelastic proton-proton interactions can be calculated with high accuracy using accelerator measurements of the inclusive cross-sections  $\sigma(E_i, E_p)$  for production of a particle  $i$  in hadronic interactions (see e.g. Gaisser 1990). The emissivity of  $\pi^0$ -mesons calculated in the  $\delta$ -functional approximation for the cross-section  $\sigma(E_\pi, E_p)$  reads

$$\begin{aligned} q_\pi(E_\pi) &= c n_H \int \delta(E_\pi - K_\pi E_{\text{kin}}) \sigma_{\text{pp}}(E_p) n_p(E_p) dE_p \\ &= \frac{c n_H}{K_\pi} \sigma_{\text{pp}} \left( m_p c^2 + \frac{E_\pi}{K_\pi} \right) n_p \left( m_p c^2 + \frac{E_\pi}{K_\pi} \right) \end{aligned} \quad (23)$$

where  $\sigma_{\text{pp}}(E_p)$  is the total cross-section of inelastic  $pp$  collisions, and  $K_\pi$  is the mean fraction of the kinetic energy  $E_{\text{kin}} = E_p - m_p c^2$  of the proton transferred to the secondary  $\pi^0$ -meson per collision;  $n_p(E_p)$  is the energy distribution of the protons.

In a broad region from GeV to TeV energies  $K_\pi \approx 0.17$  which includes also  $\sim 6\%$  contribution from  $\eta$ -meson production (Gaisser 1990). From the threshold at  $E_{\text{kin}} \simeq 0.3$  GeV,  $\sigma_{\text{pp}}$  rises rapidly to about 28–30 mb at energies about  $E_{\text{kin}} \leq 2$  GeV. After that  $\sigma_{\text{pp}}$  increases only logarithmically. For calculations we approximate

$$\sigma_{\text{pp}}(E_p) \approx 30 [0.95 + 0.06 \ln(E_{\text{kin}}/1 \text{ GeV})] \text{ mb} \quad (24)$$

for  $E_{\text{kin}} \geq 1$  GeV, and assume  $\sigma_{\text{pp}} = 0$  at lower energies. More accurate approximation of the cross-section below 1 GeV (see e.g. Dermer 1986) does not noticeably change the fluxes of  $\gamma$ -rays even at very low energies provided that the broad power-law spectrum of protons extends beyond 10 GeV, and thus the overall flux is contributed by protons with energies above few GeV.

Good accuracy of this simple approach is demonstrated in Fig. 4 where we compare the emissivity of  $\pi^0$ -decay  $\gamma$ -rays calculated on the base of Eqs. (22)–(24) with the results of the recent Monte-Carlo calculations of Mori (1997) based on a detailed treatment of the cross-sections of secondary pion production at nucleon-nucleon interactions. The full dots in Fig. 4 correspond to calculations of Mori for his ‘‘median’’ proton flux (Eq. 3 in Mori 1997). The solid line in Fig. 4 corresponds to our calculations for the same ‘‘median’’ proton flux.

The dashed curve corresponds to our calculations but for the local CR proton flux (see e.g. Simpson 1983) in the form

$$J_\odot(E_p) = 2.2(E_p/1 \text{ GeV})^{-2.75} \text{ cm}^{-2} \text{ s}^{-1} \text{ sr}^{-1} \text{ GeV}^{-1}, \quad (25)$$

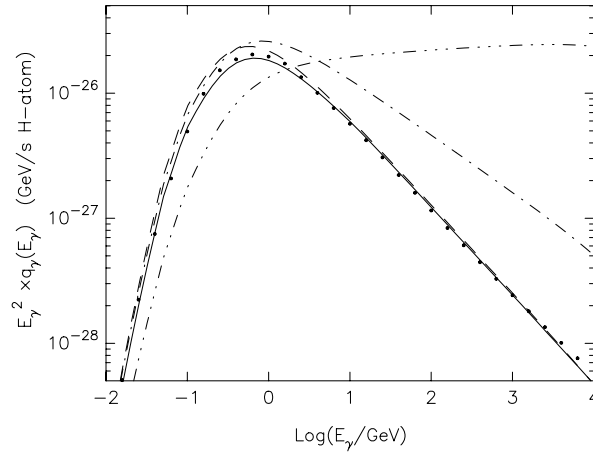


**Fig. 4.** The emissivities, per 1 H-atom, of  $\pi^0$ -decay  $\gamma$ -rays calculated using an approximate method given by Eqs. (22)–(24) for the spectra of CR protons corresponding to the ‘median’ proton flux (solid line) of Mori (1997), and the flux given by Eq. (25) (dashed line), as compared with the results of detailed emissivity calculations by Mori (1997) shown by full dots. The dot-dashed and 3-dot-dashed curves correspond to the emissivities calculated for the single power-law spectra of protons with indices  $\Gamma_p = 2.5$  and  $\Gamma_p = 2$ .

which has been used for the detailed  $\gamma$ -ray emissivity calculations by Dermer (1986). Here also we have a very good agreement; the original spectrum from Dermer (1986) is not shown in order not to overload the figure with almost coinciding curves.

Two other curves in Fig. 4 correspond to the emissivities calculated for the power law proton spectra with spectral indices  $\Gamma = 2.5$  (dot-dashed curve) and  $\Gamma = 2$  (3-dot-dashed curve), normalized to the same energy density of CR protons  $w_p = \int n_p(E_p) E_p dE_p \approx 1.2 \text{ eV/cm}^3$  derived from the CR proton flux given by Eq. (25). For CR proton spectra with  $\Gamma \geq 2.4$  the emissivities, in terms of  $E_\gamma^2 q_\gamma$ , reach the maximum at  $E \simeq 1$  GeV, and then at lower energies the spectra sharply decline. Note that we do not find any peculiarity in the declining part of the spectrum at energies between 100 MeV and 1 GeV neither in our nor in the Dermer’s (1986) or Mori’s (1997) spectra, in contrast to the apparent changes of the sign of the second derivative in the emissivity spectra presented by Pohl & Esposito (1998) and Strong et al. (2000).

#### 4.2. Fitting the GeV bump

An important feature of the  $\gamma$ -rays of nucleonic origin which allows to fill up the observed ‘bump’ of diffuse radiation at GeV energies in Fig. 3 without violation of the fluxes observed at MeV energies is a profound drop of the spectrum of this component below 100 MeV.

In Fig. 5a we show the fluxes calculated for a single power-law spectra of CR protons  $J(E_p) \propto E_p^{-\Gamma_p}$  assuming different values for  $\Gamma_p$ . All fluxes shown correspond to the product of the energy density of protons to column density of gas in the inner Galaxy  $w_p N_H = 2.5 \times 10^{22} \text{ eV/cm}^5$ . Besides, in order to take into account a contribution due to CR nuclei, hereafter

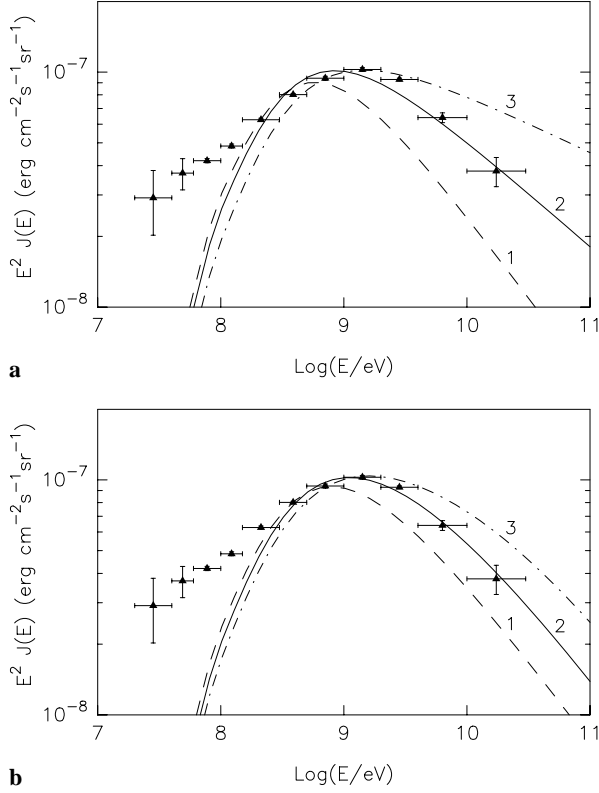


**Fig. 5a and b.** The fluxes of  $\pi^0$ -decay  $\gamma$ -rays calculated for CR proton energy distributions given in a single power-law form (**a** – top panel), and in the form of Eq. (26) (**b** – bottom panel). The fluxes in Fig. 5a are calculated assuming  $w_p N_H = 2.5 \times 10^{22}$  eV/cm<sup>5</sup> and 3 different power-law indices  $\Gamma_p$ : 2.75 (curve 1 – dashed), 2.5 (2 – solid), and 2.3 (3 – dot-dashed). The fluxes in **b** are calculated assuming  $w_p N_H = 2.1 \times 10^{22}$  eV/cm<sup>5</sup>, and the same indices  $\Gamma_0 = 2.1$  and  $\delta = 0.65$  in Eq. (26), but three different values for the characteristic energy  $E_*$ : 3 GeV (1 – dashed), 20 GeV (2 – solid), and 100 GeV (3 – dot-dashed).

the fluxes produced by CR protons are multiplied by a *constant* nuclear enhancement factor  $\eta_A = 1.5$  which takes into account the contribution from the nuclei both in CRs and ISM (Dermer 1986), although at energies above 100 GeV this factor may gradually increase (see Mori 1997).

The dashed curve in Fig. 5a shows that the flux predicted for a spectrum similar to the locally observed CR protons with the power-law index  $\Gamma_p = 2.75$ , fails to explain the diffuse  $\gamma$ -ray flux observed from the inner Galaxy at energies above 1 GeV by a factor of 1.5–2. This deficit cannot be removed by an assumption of a larger  $w_p$  or  $N_H$ , because the flux predicted at 500 MeV is already equal to the observed flux. An assumption of a very hard power law index for the CRs in the Galaxy,  $\Gamma_p = 2.3$  (dot-dashed line), explains the data at few GeV, but overpredicts the flux at higher energies. And finally, a moderately steep spectrum of protons with a power-law index  $\Gamma_p \simeq 2.5$  could explain the spectral shape of the observed ‘GeV bump’ (solid line).

There is another possibility to fit the GeV spectrum of the observed diffuse radiation by  $\pi^0$ -decay  $\gamma$ -rays. In Fig. 5b we

show the fluxes calculated for the spectra of CR protons in the form

$$n_p(E_p) \propto E_p^{-\Gamma_0} \left[ 1 + \left( \frac{E_p}{E_*} \right)^\delta \right]^{-1}. \quad (26)$$

This spectrum corresponds to the power-law index of protons  $\Gamma_p \approx \Gamma_0$  at energies below some  $E_*$ , but  $\Gamma_p \approx \Gamma_0 + \delta$  at high energies  $E_p \gg E_*$ . An energy distribution of protons of this kind is to be expected if the source function (acceleration spectrum) of accelerated protons has a single power-law form with an index  $\Gamma_0$ . Then the energy distribution of the protons, which practically do not suffer energy losses (but which nevertheless are formally taken into account in the numerical calculations), can be approximated as  $n_p(E_p) \simeq q_p(E_p) \cdot \tau_{\text{esc}}(E_p)$ . This is easily reduced to the form of Eq. (26), if the diffusive escape time of CRs from the inner Galactic disk (Eq. 8) equals the convective escape time at  $E_p = E_*$ . The results of calculations in Fig. 5b show that the GeV bump in the spectrum of diffuse radiation can be well explained (solid line) by a hard spectrum of accelerated protons with  $\Gamma_0 \simeq 2.1$  if one takes also into account the diffusive escape of particles from the galactic disk with a power law index  $\delta \sim 0.6$  resulting in a steepening of the CR spectrum above the energy  $E_* \sim 10$ –20 GeV.

The results shown in Fig. 5 demonstrate that it is possible to explain in a natural way the ‘GeV’ bump observed in the spectrum of diffuse galactic radiation by  $\pi^0$ -decay  $\gamma$ -rays assuming relatively hard spectrum of protons at energies below 100 GeV. However, the best fits in Fig. 5 do not take into account the fluxes contributed by other  $\gamma$ -ray production mechanisms, in particular by the IC radiation of the electrons. In fact, the IC fluxes are not negligible and should be taken into account for any realistic combination of parameters characterizing the ISM and CRs. In its turn, the expected IC contribution at GeV energies is tightly connected with the fluxes at lower energies, which are contributed not only by IC  $\gamma$ -rays but also by the bremsstrahlung, and possibly also by the annihilation components of radiation. Therefore, any attempt to fit the observed GeV spectrum of diffuse radiation by  $\pi^0$ -decay  $\gamma$ -rays cannot be treated separately, but rather should be conducted within the multiwavelength approach to the problem.

## 5. Overall fluxes

All radiation mechanisms considered in previous sections significantly contribute to the overall flux of the broad-band diffuse  $\gamma$ -radiation of the Galactic disk. In Fig. 6 we show that the  $\gamma$ -ray data from  $\sim 1$  MeV to 30 GeV can be well explained with a set of quite reasonable parameters both for the ISM and for the acceleration and propagation of the nucleonic and electronic components of the galactic CRs. For calculations in Fig. 6 we have assumed a mean line-of-sight depth for the inner Galactic disk  $l_d = 15$  kpc as in Fig. 2, and a column density  $N_H = 1.5 \times 10^{22}$  cm<sup>-3</sup>. This corresponds to a reasonable mean gas density along the line of sight at low galactic latitudes about  $n_H = N_H/l_d = 0.33$  cm<sup>-3</sup>. Calculations are done so that the resulting energy distributions of CR protons and electrons

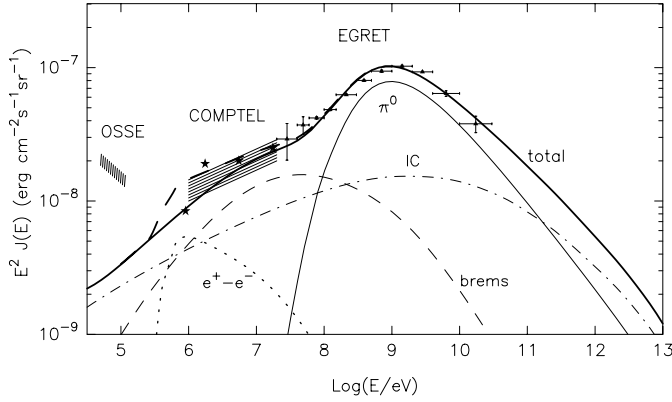


**Fig. 6.** The fluxes of diffuse radiation produced by both electronic and nucleonic components of cosmic rays in the inner Galaxy, calculated for a hard power-law source functions of the electrons with  $\Gamma_{e,0} = 2.15$ , and of the protons with  $\Gamma_{p,0} = 2.1$ , and the escape time parameters  $\delta = 0.65$ ,  $\tau_{10} = 1.4 \times 10^7$  yr,  $\tau_{\text{conv}} = 2 \times 10^7$  yr. Other model parameters are:  $w_e = 0.075$  eV/cm<sup>3</sup>,  $w_p = 1$  eV/cm<sup>3</sup>,  $N_H = 1.5 \times 10^{22}$  cm<sup>-2</sup>,  $l_d = 15$  kpc,  $B = 6$   $\mu$ G. Contributions from  $\pi^0$ -decay (thin solid line), bremsstrahlung (dashed), inverse Compton (dot-dashed), and positron annihilation in flight (dotted line, for  $C_+ = 0.5$ )  $\gamma$ -radiation mechanisms are shown. The heavy solid line shows the total flux without contribution from the positron annihilation, and the heavy dashed line takes this flux into account.

are normalized to the energy densities  $w_p = 1$  eV/cm<sup>3</sup> and  $w_e = 0.075$  eV/cm<sup>3</sup>. The latter value is larger than the energy density of the local CR electrons by a factor about 1.5 or so, depending on poorly known flux of the local CR electrons below 1 GeV. Such an enhanced energy density of CR electrons is quite possible if we take into account that the concentration of CR sources presumably increases towards the galactic centre, and that the electrons suffer significant energy losses. It is worth notice that the values of the parameters  $N_H$ ,  $l_d$ ,  $w_p$  and  $w_e$  may somewhat vary, but the spectral fits would be essentially similar to the one in Fig. 6 if the products  $N_H \times w_p$  and  $n_H \times w_e$  are kept at the same level as in Fig. 6.

In Fig. 6 hard power law source functions in the form of Eq. (11), with  $\Gamma_{e,0} = 2.15$  and  $\Gamma_{p,0} = 2.1$  for the electrons and protons respectively, are assumed. For the CR escape times in Eqs. (7) and (8) we have chosen  $\delta = 0.65$ , and  $\tau_{10} = 1.4 \times 10^7$  yr and  $\tau_{\text{conv}} = 2 \times 10^7$  yr. For these parameters the diffusive escape time at the energy  $E_* = 5.8$  GeV becomes equal to the time of convective escape, so in the energy range from a few GeV to  $\sim 10$  GeV the spectrum of CR protons (which do not practically suffer energy losses) is described by Eq. (26); it gradually steepens from the initial power-law with  $\Gamma_{p,0} = 2.1$  to  $\Gamma_p = 2.75$ . A decrease of  $E_*$ , as compared with the ‘best fit’ value  $E_* = 20$  GeV in Fig. 5b, is necessitated by the increasing contribution of IC radiation to the observed diffuse flux at energies  $E > 1$  GeV. Note that for CR proton spectra with  $\Gamma_p = \Gamma_{p,0} + \delta \leq 2.6$  this effect of gradually increasing contribution of the IC fluxes at GeV energies makes an interpretation of the observational data rather problematic, whereas without the contribution of the IC component a single

power-law spectrum of CR protons with  $\Gamma_p \simeq 2.5$  could explain the ‘GeV bump’ (see Fig. 5a).

The heavy solid curve in Fig. 6 shows the total  $\gamma$ -ray flux without the contribution from relativistic positron annihilation. In the energy region below 3 MeV the slope of this curve is noticeably flatter than the characteristic slope of the fluxes detected by COMPTEL (hatched zone; Strong et al. 1997). Meanwhile at MeV energies the flux of this annihilation radiation may significantly contribute to the overall flux, and it may even exceed the individual fluxes of both bremsstrahlung and IC  $\gamma$ -rays, provided that at energies below 100 MeV the positron content in the electronic component of the Galactic cosmic rays is significant. The dotted curve in Fig. 6 corresponds to an assumption of a high value of  $C_+ = 0.5$ , and the heavy dashed line shows the overall (“IC+bremsstrahlung+annihilation”) flux of  $\gamma$ -rays radiated by the electron component of CRs. For comparison, we show by stars also the COMPTEL data points (Hunter et al. 1997b) corrected for the contamination caused by the positronium annihilation radiation observed (Purcell et al. 1993) in the same direction. We see that the annihilation of positrons “in flight”, on top of the IC and bremsstrahlung fluxes, fits rather well the COMPTEL measurements.

Finally, in the context of principal radiation mechanisms of the diffuse galactic gamma radiation at MeV energies, we should mention also a possible contribution of the prompt  $\gamma$ -ray line emission produced by sub-relativistic cosmic rays via nuclear de-excitation. The emissivity of the total (unresolved)  $\gamma$ -ray line emission in the energy range between several hundred keV and several MeV, normalized to the energy density of sub-relativistic CRs  $w_{\text{scr}} = 1$  eV/cm<sup>3</sup>, and calculated for the standard cosmic composition (of the ambient matter and galactic CRs), is about  $2 \times 10^{-25}$  ph s<sup>-1</sup> H-atom (Ramaty et al. 1979). This implies that for  $N_H = 1.5 \cdot 10^{22}$  cm<sup>-2</sup> and  $w_{\text{scr}} \leq 1$  eV/cm<sup>3</sup>, the energy flux of this component of gamma radiation cannot exceed  $10^{-9}$  erg/cm<sup>2</sup> s ster. Therefore, this radiation mechanism could hardly be responsible for more than several per cent of the observed  $\gamma$ -ray flux at MeV energies, unless the energy density of sub-relativistic particles in the ISM significantly exceeds the “nominal” energy density of CRs in the relativistic regime,  $w_{\text{scr}} \gg w_0 \simeq 1$  eV/cm<sup>3</sup>.

Hard X-ray emission from the inner parts of the Galaxy has been recently reported by the Ginga and Welcome-1 (Yamasaki et al. 1997), RXTE (Valinia & Marshall 1998), and OSSE (Kinzer et al. 1997) teams. In Fig. 6 we show the fluxes of diffuse hard X-rays reported by OSSE. It is seen that the Bremsstrahlung + IC emission of the ‘radio’ electrons may contribute only (10–20) % to the galactic hard X-ray background. In order to explain the bulk of this radiation by the non-thermal bremsstrahlung one has to postulate an existence of the interstellar populations of sub-relativistic electrons (e.g. Yamasaki et al. 1997) and protons (e.g. Boldt 1999). It should be noted that the bremsstrahlung of sub-relativistic particles, both of electrons and protons, is a rather inefficient mechanism of radiation since due to severe ionization losses only  $\simeq 10^{-5}$  part of the kinetic energy of particles is released in the form of non-thermal hard X-rays (Aharonian et al. 1979, Skibo et al. 1996). There-

fore the “sub-relativistic bremsstrahlung” models require continuous injection of low-energy electrons and/or protons, e.g. by SNRs, into the ISM with uncomfortably large rates, especially if one tries to explain the fluxes of the low-energy X-rays,  $W_{\text{scr}} \simeq 10^{43} \text{ erg s}^{-1}$  (Skibo et al. 1996). Moreover, in the case of the proton bremsstrahlung the production of X-rays is tightly connected with the prompt  $\gamma$ -ray line emission due to the excitation of the nuclei (first of all, Fe, C, O, etc.) of the ambient gas by the same protons (Aharonian et al. 1979). Therefore this allows robust upper limits on the flux of the proton bremsstrahlung X-rays based on the observed fluxes of diffuse  $\gamma$ -rays at MeV energies. The recent analysis by Pohl (1998), based on the comparison of the observed keV and MeV fluxes leads to a conclusion that indeed the proton bremsstrahlung alone could not be responsible for the bulk of the diffuse Galactic X-ray emission.

An alternative mechanism for an explanation of the diffuse X-radiation of the galactic disc - the synchrotron emission of ultra-relativistic electrons in the interstellar magnetic fields - has been suggested by Porter & Protheroe (1997). An obvious advantage of this mechanism, compared with the bremsstrahlung of sub-relativistic particles, is its almost 100% efficiency of transformation of the kinetic energy of the electrons into the X-radiation. On the other hand this mechanism requires, for any reasonably ambient magnetic field, an efficient acceleration of electrons up to energies of 300–500 TeV.

These electrons could hardly be produced by the shocks of SNRs because of severe synchrotron losses on timescale

$$t_{\text{sy}} \approx 1.2 \cdot 10^3 (E_e/100 \text{ TeV})^{-1} (B/10 \mu\text{G})^{-2} \text{ yr}. \quad (27)$$

Comparing this time with the maximum rate of the diffusive shock acceleration (Lagage & Cesarsky 1983) in the extreme limit of Bohm diffusion, one easily finds an estimate of the maximum energy of accelerated electrons

$$E_0^{(\text{max})} \simeq 90 \left( \frac{B}{10 \mu\text{G}} \right)^{-1/2} \left( \frac{v_s}{4000 \text{ km s}^{-1}} \right) \text{ TeV}, \quad (28)$$

where  $v_s$  is the shock speed. Thus, for typical parameters of a SNR in a stage close to its Sedov phase, when the acceleration of the bulk of relativistic particles takes place (e.g. Berezhko & Völk 1997), namely  $v_s \leq 4000 \text{ km s}^{-1}$  and  $B \geq 5 \mu\text{G}$ , the characteristic maximum energy of accelerated electrons cannot significantly exceed 100 TeV.

More probable sites for acceleration of electrons to energies  $\gg 100 \text{ TeV}$  could be the shocks terminating relativistic winds driven by pulsars. For example, it is widely believed that the electrons in the Crab Nebula are accelerated at the termination shock of the pulsar wind to energies  $\sim 10^{15} \text{ eV}$  (see e.g. Arons 1996). An assumption that electrons could be accelerated well beyond 100 TeV at the wind termination shocks of much older pulsars could then explain the diffuse hard X-ray background radiation of the Galaxy as a synchrotron emission of these electrons. The life time of  $E_e \sim 300 \text{ TeV}$  electrons does not exceed several hundred years, therefore they cannot propagate a distance more (and probably even much less) than a few tens of parsec from their acceleration sites. It means that the synchrotron origin of the galactic diffuse X-ray background

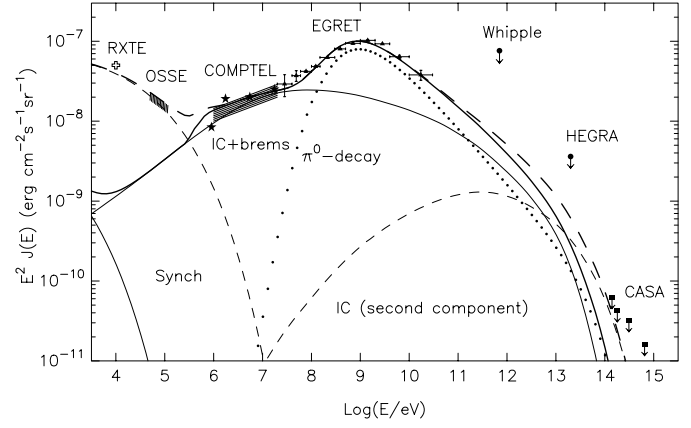


**Fig. 7.** The diffuse background radiation from the Galactic plane corresponding to the two-component model for the relativistic electrons. The heavy solid line corresponds to the fluxes produced by the electrons of the first (main) population, with the same model parameters as in Fig. 6, but for  $\delta = 0.7$  and  $C_+ = 0.3$ , and the heavy dashed line shows the overall fluxes including the contribution from the second (“pulsar wind”- see text) population of electrons accelerated to energies  $E_0 = 250 \text{ TeV}$ . The local mean magnetic field for the second electron population is  $B_2 = 25 \mu\text{G}$ . Besides the galactic diffuse background  $\gamma$ -radiation detected by COMPTEL and EGRET, the X-ray backgrounds detected by RXTE (Valinia & Marshall 1998) and OSSE (Kinzer et al. 1997), as well as the upper flux limits at very high energies (VHE) reported by Whipple, HEGRA, and CASA-MIA collaborations are also shown.

would be possible only in a form of *superposition* of the emission from a number of unresolved weak and *continuous* sources along the line of sight. These conditions could be satisfied e.g. by  $10^5 - 10^6 \text{ yr}$  old pulsars, the overall number of which in the inner Galaxy could be estimated up to  $\sim 3 \times 10^4$  if neutron stars are produced with a rate of about 1 per 30 yrs.

In Fig. 7 we show the broad band diffuse radiation flux calculated in the framework of the model which assumes that besides the main population of CRs (presumably accelerated by the SNR shocks), there is also a second population of electrons accelerated well beyond 100 TeV at the pulsar wind termination shocks of old neutron stars/pulsars in the inner Galaxy. The parameters for the first (main) population of accelerated particles, both the electrons and protons, are essentially the same as in Fig. 6 (except for  $\delta = 0.7$  and  $C_+ = 0.3$  used in Fig. 7). For the second electron population we assume an acceleration spectrum with  $\Gamma_e = 2$  and an exponential cutoff energy  $E_0 = 250 \text{ TeV}$ , but also a turnover of the spectrum at energies below 1 TeV. Note that such a turnover at low energies is a characteristic feature of the electrons accelerated at the pulsar wind termination shocks (see e.g. Arons 1996), which however does not affect the overall flux of diffuse  $\gamma$ -rays below TeV energies (dominated by the radiation of the main component of CRs). For the mean magnetic field of the ISM in Fig. 7 we assume the same value as in Fig. 6,  $B = B_1 = 6 \mu\text{G}$ . But for the second electron component we assume significantly larger ambient field,  $B_2 = 25 \mu\text{G}$ , in order to fit the hard X-ray data. Different magnetic fields for the first and second components of the synchrotron radiation

can be understood if we remember that the multi-TeV electrons cool very rapidly therefore they cannot propagate very far from their accelerators. More specifically, the hypothesis that the *second* (ultra-high energy) population of electrons is produced at the termination shocks of relativistic pulsar winds (which inject not only relativistic electrons, but also magnetic fields) could explain also why the magnetic field  $B_2$  could be much higher than the mean field  $B_1$  in the Galaxy.

The assumption of high magnetic field  $B_2$  becomes very important for a self-consistent interpretation of the ‘diffuse’ flux of hard X-rays detected in the galactic plane in terms of synchrotron radiation of  $E_e \geq 300$  TeV electrons, because otherwise the fluxes of IC radiation produced by the same electrons would exceed the upper flux limits reported by CASA-MIA collaboration at energies  $E_\gamma \geq 100$  TeV (Barione et al. 1998). As it is seen in Fig. 7, the energy flux of OSSE exceeds the flux upper limits of CASA by a factor of  $\geq 300$ . The ratio of energy fluxes of synchrotron to IC radiations produced by an electron is about the ratio of the magnetic field to the soft photon field energy densities, i.e.  $(B^2/8\pi)/0.25 \text{ eV/cm}^3 = 10(B/10 \mu\text{G})^2$ , if the IC scattering occurs in the Thomson limit, when the parameter  $b = 4\epsilon_0 E_e / (m_e c^2)^2 \ll 1$  ( $\epsilon_0 \sim 6.5 \times 10^{-4} \text{ eV}$  is the mean energy of 2.7 KMBR photons). Actually, the IC scattering of  $E_e \sim 300$  TeV electrons occurs in a moderate Klein-Nishina regime with  $b \sim 3$ . For these values of parameter  $b$  the emissivity of IC radiation is reduced (compared with the Thomson limit) by a factor 5–10, therefore the ratio of the synchrotron to IC fluxes  $\geq 300$  implies a magnetic field  $B_2 \geq 20 \mu\text{G}$ .

The acceleration power in the second electron component which is needed for interpretation of the hard X-ray background in Fig. 7 is about  $6 \times 10^{36} \text{ erg s}^{-1}$  per  $\text{kpc}^3$ , or about  $L_e^{(\text{II})} \simeq 1.4 \times 10^{39} \text{ erg s}^{-1}$  in the entire inner galactic disk with a radius about 8 kpc and a thickness  $h \simeq 1 \text{ kpc}$ . For the overall number of such pulsars of order  $3 \times 10^4$ , this implies a rather modest mean acceleration power per 1 ‘old pulsar’ of about  $5 \times 10^{34} \text{ erg s}^{-1}$ , i.e. by four orders of magnitude less than the power of the relativistic electron-positron wind of the Crab pulsar. Note that the kick velocities of the pulsars can be of order from a few 100 to  $\sim 1000 \text{ km s}^{-1}$ , so the  $10^6$  yr old pulsars would be able to propagate to distances  $\leq (0.3-1) \text{ kpc}$ , contributing therefore to the emission at the galactic latitudes up to several degree. Note also that even for  $10^4$  pulsars in the  $10^\circ \times 90^\circ$  field of view of the inner Galaxy considered here, the mean density of such pulsars on the sky corresponds to  $\simeq 10$  per square degree. Therefore in principle for the hard X-ray/soft  $\gamma$ -ray detectors, which typically do not have an excellent angular resolution, a superposition of the emission of large number of such relatively weak sources (with sizes presumably  $\geq 10 \text{ pc}$ ) in the field of view of the detector could imitate a “diffuse” emission.

## 6. Discussion

The diffuse galactic gamma ray emission carries a unique information, a proper understanding of which would eventually result in a quantitative theory of the origin of galactic cosmic rays.

Although the problem is essentially complicated and confused because of several competing mechanisms of production of diffuse  $\gamma$ -rays, the data obtained by the COMPTEL and EGRET detectors aboard Compton GRO allow rather definite conclusions concerning the relative contributions of different  $\gamma$ -ray production mechanisms in the energy region from 1 MeV to 30 GeV.

At energies below 100 MeV the diffuse  $\gamma$ -radiation has an electronic origin. For a set of reasonable parameters for both the ISM and CR electrons, the observed  $\gamma$ -ray fluxes from 10 MeV to 100 MeV can be well explained by the superposition of the bremsstrahlung and the IC components of radiation of relativistic electrons. At lower energies, a non-negligible flux can be contributed by the annihilation of relativistic positrons with the ambient thermal electrons. Moreover, if the content of positrons at energies  $E \leq 10 \text{ MeV}$  is close to  $e^+/(e^- + e^+) \sim 0.5$ , the  $\gamma$ -ray flux around 1 MeV would be dominated by the non-thermal annihilation radiation. Between several MeV and 100 MeV the radiation is dominated by the electron bremsstrahlung. This result agrees with previous studies (Kniffen & Fichtel 1981, Sacher & Schönfelder 1984, Gehrels & Tueller 1993).

Above 100 MeV the IC process dominates in the production of diffuse  $\gamma$ -rays, but at these energies a new mechanism is needed in order to explain the so called “GeV bump” detected by EGRET. We believe that this distinct emission feature of the inner Galaxy could be naturally explained by  $\gamma$ -rays of nucleonic origin produced at the interactions of CR protons and nuclei with the ambient interstellar gas. Indeed, the overall observed MeV/GeV emission of the inner Galaxy is well fitted by the  $\pi^0$ -decay  $\gamma$ -rays (on top of “IC + bremsstrahlung + annihilation” contribution by CR electrons) provided that the spectrum of CR protons in the inner galactic disk at low energies is substantially flatter than the spectrum of directly observed local CRs. In particular, a proton spectrum in the form of Eq. (26) with  $E_* \sim 10 \text{ GeV}$ ,  $\Gamma_0 = 2.1$  and  $\delta \simeq 0.6$ , which could be formed due to a reasonable combination of diffusive and convective escape time-scales of CRs from the inner galactic disk, is able to explain very well the observed diffuse galactic  $\gamma$ -ray spectrum (see Fig. 6 and Fig. 7). It is interesting to note that in the total “ $\pi^0$ +IC” spectrum the contribution of  $\pi^0$ -decay  $\gamma$ -ray component gradually decreases since the spectrum of CR protons at high energies with an index  $\Gamma_p \approx \Gamma_0 + \delta \simeq 2.7$  is steeper than the spectrum of the diffuse gamma radiation with a power-law index  $\simeq 2.5$  observed at energies above several GeV. However, this decline is compensated by the hard IC component of radiation which at energies above 30 GeV becomes the dominant contributor to the overall  $\gamma$ -ray flux. For convenience of further discussion, we will call this possibility for explanation of the GeV bump in the observed  $\gamma$ -ray spectrum the scenario 1.

Another possibility for explanation of the spectrum of  $\gamma$ -rays up to 30 GeV could be a single power-law spectrum of CR protons with  $\Gamma_p \sim 2.5$ , but then we should assume a significant reduction of the IC contribution to the overall  $\gamma$ -ray flux at such high energies. This possibility, which we call the scenario 2, can be realized if the acceleration spectrum of CR electrons does not extend to TeV energies. In this scenario the

$\gamma$ -ray fluxes below several GeV are explained, as in the scenario 1, by superposition of the electronic and nucleonic components of radiation. However at higher energies the  $\gamma$ -ray flux would be strongly dominated by  $\pi^0$ -decay component of radiation. For the acceleration spectrum of protons with  $\Gamma_0 \sim 2.1$ , the required single power-law spectrum of protons in the inner Galaxy with  $\Gamma_p \sim 2.5$  could be formed if  $\delta \sim 0.4$  and  $E_* \ll 10$  GeV (see Eq. 26). This conclusion would imply that the mean time of convective escape of CRs from the disk is much larger than the diffusive escape of particles at 10 GeV.

These two scenarios predict essentially different origin of  $\gamma$ -rays in the VHE domain. While in the scenario 1 the  $\gamma$ -ray background of the galactic disk at  $E \geq 100$  GeV is contributed mainly by IC scattering of multi TeV electrons on 2.7 K MBR, in the scenario 2 the VHE  $\gamma$ -ray flux is dominated by  $\pi^0$ -decay  $\gamma$ -rays. Therefore the future spectroscopic measurements of the diffuse radiation of the inner Galaxy at low ( $|b| \leq 2^\circ$ ) and high (e.g.  $2^\circ \leq |b| \leq 10^\circ$ ) galactic latitudes by GLAST at  $E \leq 100$  GeV, and by imaging atmospheric Cherenkov telescope arrays H.E.S.S. and CANGAROO-3 (both to be located in the Southern Hemisphere) above 100 GeV could provide crucial information about the character of propagation of TeV cosmic rays in the galactic disk (Weekes et al. 1997).

Because all target photon fields for production of IC  $\gamma$ -rays extend practically with the same intensity (see e.g. Chi & Wolfendale 1991) well above the characteristic height  $h \sim 200$  pc of the gaseous disk, and since the fluxes of very high energy electrons above the galactic plane up to several hundred pc could be still significant, the realization of the scenario 1 can be distinguished from the scenario 2 by different spectra of high energy radiation detected at different galactic latitudes  $|b|$ . In particular, the scenario 1 predicts an increase of the relative contribution of the IC component to the  $\gamma$ -ray flux, therefore we should expect some flattening (depending on the rate of decline of VHE electron fluxes above the galactic plane) of the spectrum of  $\gamma$ -rays at  $|b|$  larger than few degree. Note, however, that the measurements at different  $|b|$  could not distinguish between the scenario 2, which interprets the observed Galactic ‘excess’ GeV radiation in terms of truly diffuse emission of (mainly) nucleonic origin from the models interpreting this radiation as a superposition of contributions from unresolved SNRs (Völk 1999, Berezhko & Völk 2000), or “active” molecular clouds (Aharonian 1991, Aharonian & Atoyan 1996). The level of contamination of the *truly diffuse* radiation of the disk by faint, but numerous  $\gamma$ -ray sources could be properly estimated only by future measurements of the angular distribution of the galactic background in scales less than  $1^\circ$ . The GLAST with its angular resolution as good as  $0.1^\circ$  and detection area by a factor of 10 larger than EGRET (see e.g. Bloom 1996), is nicely suited for this task.

The fluxes of  $\gamma$ -rays expected above 1 TeV in both scenarios 1 and 2 are below the current flux upper limits set by the Whipple (Reynolds et al. 1993), HEGRA (Schmele 1998) and CASA-MIA groups (see Fig. 8). However larger fluxes at such high energies cannot be excluded. Indeed, besides the hard  $\pi^0$ -decay  $\gamma$ -ray component due to CR sources which could remain unre-

solved, we may expect also higher IC fluxes of  $\gamma$ -rays radiated by a possible second component of ultra high energy electrons with a spectrum extending well beyond 100 TeV. The existence of such a component of electrons is needed within the model which interprets the hard X-radiation of the inner galactic disk as a result of synchrotron radiation of ultra-relativistic electrons. This hypothesis requires a very large (up to  $E_{\max} \sim 10^{15}$  eV) maximum energy of electrons and large magnetic field  $B_2 \geq 20 \mu\text{G}$  in order to fit the observed X-ray fluxes, as well as to avoid an overproduction of IC  $\gamma$ -rays at 100 TeV. Such large values of both  $E_{\max}$  and  $B_2$  could be probably explained assuming that this energetic component of electrons is produced at the wind termination shocks of the ensemble of old pulsars/neutron stars in the galactic disk. The hypothesis of the synchrotron origin of hard diffuse X-radiation of the galactic disk needs further confirmation based on the detailed study of spectral and spatial distribution of hard X-rays by future satellite missions like ASTRO-E and INTEGRAL, as well as by a detection of the diffuse  $\gamma$ -ray background of the galactic disk at  $E \sim 100$  TeV at the flux level rather close to the current CASA-MIA upper limits.

*Acknowledgements.* We thank the anonymous referee for his very helpful and important comments. The work of AMA has been partly supported through the Verbundfoeschung Astronomie/Astrophysik of the German BMBF under grant No. 05-2HD66A(7).

## References

- Aharonian F.A., Kelner S.R., Kotov Yu.D., 1979, In: Proc. 16th Intern. Cosmic Ray Conf., Kyoto, vol. 1, p. 173; p. 179  
 Aharonian F.A., Atoyan A.M., 1981a, SvA Lett. 7, 395  
 Aharonian F.A., Atoyan A.M., 1981b, Physics Letters 99B, 301  
 Aharonian F.A., Kirillov-Ugryumov V.G., Kotov Y.D., 1983, Astrophysics 19, 82  
 Aharonian F.A., 1991, Ap&SS 180, 305  
 Aharonian F.A., Atoyan A.M., 1996, A&A 309, 917  
 Aharonian F.A., Atoyan A.M., Völk H.J., 1995, A&A 294, L41  
 Arons J., 1996, Space Sci. Rev. 75, 235  
 Atoyan A.M., Aharonian F.A., Völk H.J., 1995, Phys. Rev. D. 52, 3265  
 Berezhko E.G., Völk H.J., 1997, Astroparticle Physics 7, 183  
 Berezhko E.G., Völk H.J., 2000, ApJ in press  
 Berezhinsky V.S., Bulanov S.V., Ginzburg V.L., Dogiel V.A., 1990, Astrophysics of Cosmic Rays. North-Holland, Amsterdam  
 Berezhinsky V.S., Gaisser T.K., Halzen F., Stanev T., 1993, Astropart. Phys. 1, 281  
 Bertsch D.L., Dame T.M., Fichtel C.E., et al., 1993, ApJ 416, 587  
 Bloemen J.B.G.M., 1987, ApJ 322, 694  
 Bloemen J.B.G.M., 1989, ARA&A 29, 469  
 Bloemen J.B.G.M., Dogiel V.A., Dorman V.L., Ptuskin V.S., 1993, A&A 267, 372  
 Bloom E.D., 1996, Space Sci. Rev. 75, 109  
 Boldt E., 1999, astro-ph/9902040; to be published in Astrophysical Lett & Communications  
 Borione A., Catanese M.A., Chantell M.C., et al., 1998, ApJ 493, 175  
 Breitschwerdt D., McKenzie J.F., Völk H.J., 1993, A&A 269, 54  
 Chi X., Wolfendale A.W., 1991, J. Phys. G 17, 987  
 Dermer C., 1986, A&A 157, 223  
 Dickey J.M., Lockman F.J., 1990, ARA&A 28, 215

- Erlykin A.D., Lipski M., Wolfendale A.W., 1998, *Astroparticle Physics* 8, 283
- Fanslow J.L., Hartman R.C., Hildebrand R.H., Meyer P., 1969, *ApJ* 158, 771
- Fathoohi L.J., Giller M, Wdowczyk J., Wolfendale A.W., Zhang L., 1995, *J. Phys. G* 21, 487
- Fichtel C.E., Hartmann R.C., Kniffen D.A., et al., 1975, *ApJ* 198, 163
- Gaisser T.K., 1990, *Cosmic rays and particle physics*. Cambridge University Press
- Gehrels N., Tueller J., 1993, *ApJ* 407, 597
- Giller M., Wdowczyk J., Wolfendale A.W., Zhang L., 1995, *J. Phys. G* 21, 487
- Ginzburg V.L., Syrovatskii S.L., 1964, *Origin of Cosmic Rays*, Pergamon Press, London
- Ginzburg V.L., 1979, *Theoretical Physics and Astrophysics*. Pergamon Press, Oxford
- Gralewicz P., Wdowczyk J., Wolfendale A.W., Zhang L., 1997, *A&A* 318, 925
- Harding A.K., Ramaty R., 1987, In: *Proc. 20th Int. Cosmic Ray Conf.* vol. 2, p. 92
- Hunter S.D., Bertsch J.R., Catelli J.R., et al., 1997a, *ApJ* 481, 205
- Hunter S.D., Kinzer R.L., Strong A.W., 1997b, In: *Dermer C.D., Strickman M.S., Kurfes J.D. (eds.) AIP Conf. Proc. 410, 4th Compton Symposium*, AIP, New York, p. 192
- Kinzer R.L., Purcell W.R., Johnson W.N., et al., 1996, *A&AS* 120, 317
- Kinzer R.L., Purcell W.R., Kurfess J.D., et al., 1997, In: *Dermer C.D., Strickman M.S., Kurfes J.D. (eds.) AIP Conf. Proc. 410, 4th Compton Symposium*, AIP, New York, p. 1193
- Kniffen D.A., Fichtel C.E., 1981, *ApJ* 250, 389
- Lagage P.O., Cesarsky C.J., 1983, *A&A* 118, 223
- Lerche I., Schlickeiser R., 1980, *A&A* 239, 1089
- Lerche I., Schlickeiser R., 1982, *A&A* 107, 148
- Leventhal M., 1973, *ApJ* 183, L147
- Mathis J.S., Mezger P.G., Panagia N., 1983, *A&A* 128, 212
- Mayer-Hasselwander H.A., Kaubach G., Bennet K., et al., 1982, *A&A* 105, 164
- Mori M., 1997, *ApJ* 478, 225
- Moskalenko I.V., Strong A.W., 2000, *ApJ* 528, 357
- Nishimura J., Fujii M., Taira T., et al., 1980, *ApJ* 238, 394
- Owens A.J., Jokipii J.R., 1977, *ApJ* 215, 685
- Pohl M., 1998, *A&A* 339, 587
- Pohl M., Esposito J.A., 1998, *ApJ* 507, 327
- Porter T.A., Protheroe R.J., 1997, *J. Phys. G* 23, 1765
- Purcell W.R., Grabelsky D.A., Ulmer M.P., et al., 1993, *ApJ* 413, L85
- Ramana Murthy P.V., Wolfendale A.W., 1993, *Gamma-Ray Astronomy*. Cambridge University Press
- Ramaty R., Kozlovsky B., Lingenfelter R.E., 1979, *ApJS* 40, 487
- Reynolds P.T., Akerlof C.W., Cawley M.F., et al., 1993, *ApJ* 404, 206
- Sacher W., Schönfelder V., 1984, *ApJ* 297, 817
- Simpson J.A., 1983, *Ann. Rev. Nucl. Part. Phys.* 33, 323
- Schmele D., 1998, *Dissertation, Universität Hamburg (Hamburg)*
- Skibo J.G., Ramaty R., Purcell W.R., 1996, *A&AS* 120, 403
- Stecker F.W., 1970, *Ap&SS* 6, 377
- Strong A.W., Diehl R., Schönfelder V., et al., 1997, In: *Dermer C.D., Strickman M.S., Kurfes J.D. (eds.) AIP Conf. Proc. 410, 4th Compton Symposium*, AIP, New York, p. 1198
- Strong A.W., Moskalenko I.V., Reimer O., 2000, *ApJ* 537, 763
- Swordy S., 1993, In: *Leahy D.A., et al. (eds.) Proc. 23-th ICRC, Calgary Invited, Rapporteur and Highlight Papers*, p. 243
- Taira T., Nishimura J., Fujii M., et al., 1993, In: *Leahy D.A., et al. (eds.) Proc. 23-th ICRC, Calgary Invited, Rapporteur and Highlight Papers*, p. 128
- Valinia A., Marshall F.E., 1998, *ApJ* 505, 134
- Völk H.J., 1999, In: *Proc. GeV-TeV Astrophysics: Toward a Major Atmospheric Cherenkov Telescope VI, Snowbird, Utah*, in press
- Webber W.R., Simpson G.A., Cane H.V., 1980, *ApJ* 236, 448
- Weekes T.C., Aharonian F.A., Fegan D.J., Kifune T., 1997, In: *Dermer C.D., Strickman M.S., Kurfes J.D. (eds.) AIP Conf. Proc. 410, 4th Compton Symposium*, AIP, New York, p. 361
- Yamasaki N.Y., Ohashi T., Takahara F., et al., 1997, *ApJ* 481, 821
- Zirakashvili V. N., Breitschwerdt D., Ptuskin V.S., Völk H.J., 1996, *A&A* 311, 113